

On lead-lag estimation of non-synchronously observed point processes

Takaaki Shiotani*

Takaki Hayashi[†]

Yuta Koike*

January 6, 2026

Abstract

This paper introduces a new theoretical framework for analyzing lead-lag relationships between point processes, with a special focus on applications to high-frequency financial data. In particular, we are interested in lead-lag relationships between two sequences of order arrival timestamps. The seminal work of Dobrev and Schaumburg proposed model-free measures of cross-market trading activity based on cross-counts of timestamps. While their method is known to yield reliable results, it faces limitations because its original formulation inherently relies on discrete-time observations, an issue we address in this study. Specifically, we formulate the problem of estimating lead-lag relationships in two point processes as that of estimating the shape of the cross-pair correlation function (CPCF) of a bivariate stationary point process, a quantity well-studied in the neuroscience and spatial statistics literature. Within this framework, the prevailing lead-lag time is defined as the location of the CPCF’s sharpest peak. Under this interpretation, the peak location in Dobrev and Schaumburg’s cross-market activity measure can be viewed as an estimator of the lead-lag time in the aforementioned sense. We further propose an alternative lead-lag time estimator based on kernel density estimation and show that it possesses desirable theoretical properties and delivers superior numerical performance. Empirical evidence from high-frequency financial data demonstrates the effectiveness of our proposed method.

Keywords: Bandwidth selection; cross-correlation histogram; cross-pair correlation function; high-frequency data; non-synchronicity; lead-lag effect.

1 Introduction

Empirical research on lead-lag relationships between two financial time series has long been an active area of study in finance. Their identification is fundamental to understanding price discovery and may provide practitioners with opportunities for excess profits. In modern financial markets, such relationships can persist only over very short horizons, even on the order of one millisecond or less. Therefore, lower-frequency or coarsely aggregated data inevitably fail to find the fine structure of these relationships. This motivates the use of *tick data*, i.e., raw high-frequency data that records all transactions as they arrive randomly and *non-synchronously*. In particular, handling non-synchronicity is a central issue when estimating lead-lag relationships from such data.

*Graduate School of Mathematical Sciences, The University of Tokyo, 3-8-1 Komaba, Meguro-ku, Tokyo 153-8914 Japan

[†]Graduate School of Business Administration, Keio University, 4-1-1 Hiyoshi, Yokohama 223-8526, Japan

Most existing studies have examined high-frequency lead-lag dynamics using price series. Prominent approaches include methods based on estimating the cross-covariance function [26, 43, 45], wavelet analysis [38, 39], local spectral estimation [50], Hawkes process-based multi-asset models [5, 22] and the multi-asset lagged adjustment model of [16]. Among these, Hoffmann *et al.* [43] introduced a simple cross-covariance estimator that can be computed directly from non-synchronously observed returns and proposed estimating the prevailing lead-lag time by locating its maximizer. Although their method yields sensible empirical implications due to its intuitive interpretation [2, 7, 10, 25, 45, 59], the resulting lead-lag time estimates are often unstable and unreliable [7, 37, 45], presumably because high-frequency price series are affected by market microstructure noise. As an alternative method, Dobrev & Schaumburg [27] proposed model-free measurements of the lead-lag relationship between two assets based on cross-counts of their order arrivals. Their estimator of lead-lag time has been shown to produce highly stable and reliable estimates in practice; see [27, 37].

However, the Dobrev–Schaumburg method is essentially descriptive, and it is not immediately clear what underlying quantity the method actually estimates.¹ Indeed, as we show in Section 2, there exist situations in which their method performs poorly in practice, particularly when the data contain relatively few observations. Moreover, implementing their method requires partitioning the observation period into equi-spaced buckets, and the choice of bucket size has a substantial impact on the results. Yet, because the method is “model-free,” it does not offer a statistical explanation for why such sensitivity arises.

To address these issues, we reformulate the Dobrev–Schaumburg method from a point process perspective. This viewpoint reveals that their measurements essentially estimate shape characteristics of the *cross-pair correlation function* (CPCF) of a bivariate point process generated by order arrivals; see Section 3 for definitions. Accordingly, the Dobrev–Schaumburg estimator of lead-lag time can be interpreted as an estimator of the CPCF’s sharpest peak location. This interpretation also clarifies that the instability observed in their method arises when the bucket size is chosen too small relative to a range that is permissible given the properties of the underlying data. At the same time, because their estimator can only take values that are integer multiples of the bucket size, using a larger bucket size results in excessively coarse estimates. To overcome these limitations, we propose a nonparametric, kernel-based estimator of the lead-lag time, together with a data-driven bandwidth selection procedure. We show both theoretically and empirically that this new estimator produces stable and accurate results even in settings where the Dobrev–Schaumburg method fails.

The remainder of the paper is organized as follows. Section 2 provides a detailed explanation of the Dobrev–Schaumburg method. Section 3 introduces a point process framework that clarifies the theoretical meaning of the Dobrev–Schaumburg method. Section 4 proposes an alternative estimator of the lead-lag time within this framework and develops its theoretical properties. Section 5 demonstrates its superior numerical performance through a comprehensive Monte Carlo study. Section 6 presents an empirical application that illustrates the effectiveness of our proposed estimator using real data. Section 7 concludes by summarizing

¹ Although [28] discuss some asymptotic properties of their measurements when the two timestamp series are independent, they do not clearly specify the underlying estimands.

our main contributions and discussing directions for future research. The appendix contains mathematical proofs and additional implementation details.

Notation The cardinality of a finite set S is denoted by $|S|$. Leb denotes the Lebesgue measure. The Borel σ -algebra of a topological space S is denoted by $\mathcal{B}(S)$. For a real-valued function f defined on a set S , we set $\|f\|_\infty = \sup_{x \in S} |f(x)|$. Also, we denote by $\arg \max_{x \in S} f(x)$ the set of maximizers of f on S . For a random variable X and $p \geq 1$, we set $\|X\|_p := (\mathbb{E}[|X|^p])^{1/p}$. The underlying probability space is denoted by $(\Omega, \mathcal{F}, \mathbb{P})$. We interpret $1/0 = \infty$ by convention.

2 The Dobrev–Schaumburg method

Suppose that we have tick data for two financial assets, with timestamps given by $0 \leq t_1^1 < \dots < t_{n_1}^1 \leq T$ and $0 \leq t_1^2 < \dots < t_{n_2}^2 \leq T$. Throughout the paper, we assume that $T \geq 1$ is an integer and timestamps are expressed in seconds when working with real data.; hence we may regard T as a large integer. Dobrev & Schaumburg [27] proposed measuring the lead-lag relationship between two assets using the following procedure.

First, divide the observation interval $[0, T]$ into equi-spaced time buckets $I_k^h := (kh, (k+1)h]$, $k = 0, 1, \dots, T/h - 1$, where $h > 0$ is chosen so that $h^{-1} \in \mathbb{N}$. We interpret a situation where an event for asset 2 occurs with a lag $\ell \in \mathbb{Z}$ after an event for asset 1 as the existence of timestamps t_i^1, t_j^2 and a bucket index $k \in \{|\ell|, |\ell| + 1, \dots, T/h - 1 - |\ell|\}$ such that $t_i^1 \in I_k^h$ and $t_j^2 \in I_{k+\ell}^h$. By calculating the number of such bucket indices, we obtain a measure of the lead-lag effect of asset 1 on asset 2 with lag ℓ . Based on this idea, Dobrev & Schaumburg [27] introduced the *raw cross-market activity* at offset ℓ as

$$\mathcal{X}_h^{\text{raw}}(\ell) := \sum_{k=|\ell|}^{T/h-1-|\ell|} 1_{\{\exists t_i^1 \in I_k^h, \exists t_j^2 \in I_{k+\ell}^h\}}.$$

To adjust the degree of freedom, they also defined the *relative cross-market activity* as

$$\mathcal{X}_h^{\text{rel}}(\ell) := \frac{\mathcal{X}_h^{\text{raw}}(\ell)}{\min \left\{ \sum_{k=|\ell|}^{T/h-1-|\ell|} 1_{\{\exists t_i^1 \in I_k^h\}}, \sum_{k=|\ell|}^{T/h-1-|\ell|} 1_{\{\exists t_{i+\ell}^2 \in I_k^h\}} \right\}}.$$

Computing $\mathcal{X}_h^{\text{raw}}(\ell)$ and $\mathcal{X}_h^{\text{rel}}(\ell)$ requires choosing a value of h . In [27], h is set to 1 millisecond, which is chosen in an ad-hoc manner by considering the time granularity of the data. Here, 1 millisecond is the minimum time unit available in their dataset for the S&P 500 cash market.

By definition, the larger value of $\mathcal{X}_h^{\text{rel}}(\ell)$ indicates a stronger lead-lag effect in which asset 2 follows asset 1 after a delay of ℓh . Motivated by this, Dobrev & Schaumburg [27] proposed identifying the prevailing lead-lag time by locating the peak of the map $\ell \mapsto \mathcal{X}_h^{\text{rel}}(\ell)$. Specifically, given a search grid \mathcal{G}_h , the lead-lag time is estimated by

$$\hat{\theta}_h^{DS} = \hat{\ell}h, \quad \text{where } \hat{\ell} \in \arg \max_{\ell \in \mathcal{G}_h} \mathcal{X}_h^{\text{rel}}(\ell).$$

We refer to $\hat{\theta}_h^{DS}$ as the *DS estimator*. In what follows, we assume the true lead-lag time lies within the interval $(-r, r)$ for some known positive constant r , and define $\mathcal{G}_h := \{\ell \in \mathbb{Z} : |\ell h| \leq r\}$.

As mentioned in the introduction, several empirical studies have reported that the DS estimator yields stable and interpretable estimates of lead-lag time. However, there are cases where the estimator performs poorly, particularly when the dataset contains relatively few observations. Fig. 1 illustrates this issue, showing the relative cross-market activity measure computed from best-quote updates on two U.S. stock exchanges, NASDAQ and BATS, for the MNST stock on August 12, 2015. In this example, the values of the cross-market activity measure fluctuate heavily, making it difficult to identify the peak reliability. Yet, due to the “model-free” nature of the Dobrev–Schaumburg method, no statistical interpretation is provided for the origin of such instability. One goal of this study is to establish a theoretical foundation for their approach and fill this gap.

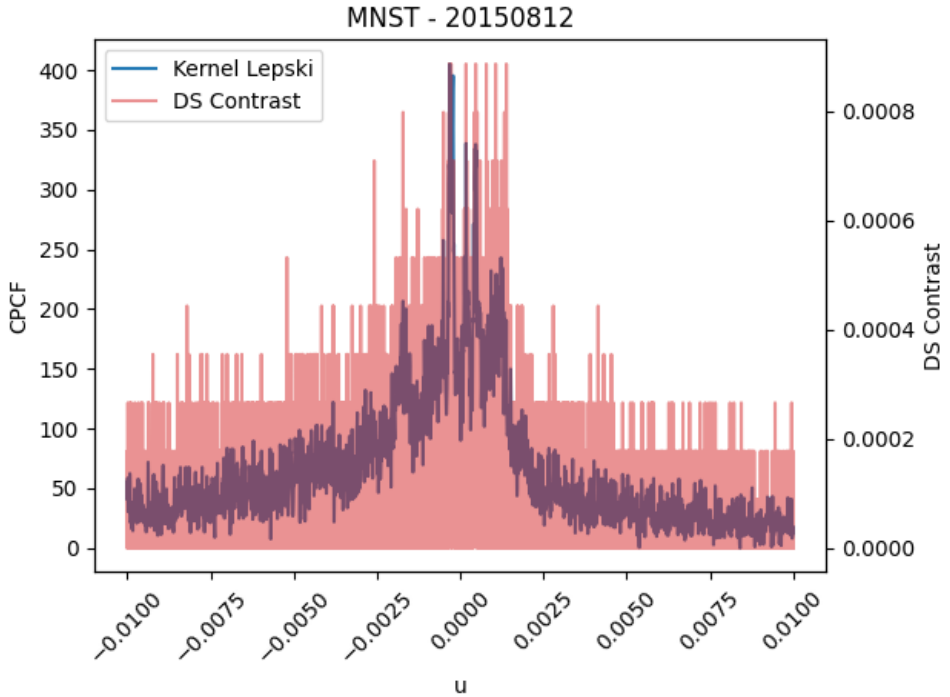


Figure 1: Contrast functions: DS vs ours. MNST, NASDAQ vs BATS (quote, Aug. 12, 2015). The cross-market activity measure $\mathcal{X}_h^{\text{rel}}(\ell)$ is indicated by the red line, while the kernel density estimator $g_h(u)$ with the Lepski-selected bandwidth (see Section 4) is indicated by the blue line. The unit of the horizontal axis is seconds.

3 Proposed framework

To clarify the statistical meaning of the Dobrev–Schaumburg method, we model the observed timestamps $(t_i^1)_{i=1}^{n_1}$ and $(t_j^2)_{j=1}^{n_2}$ as realizations of a bivariate point process on the real line. Specifically, for each $a = 1, 2$, we consider the timestamps (t_i^a) to be a result of observing a point process N_a on \mathbb{R} over the interval $[0, T]$. That is, $N_a(A) = |\{i : t_i^a \in A\}|$ for a Borel set $A \subset [0, T]$. Here and below, we mainly follow the mathematical formulation of point processes described in [23, 24] and refer to these monographs for unexplained concepts and notation (see also [65, Section 2.2] for a summary). With this formulation, we can

rewrite $\mathcal{X}_h^{\text{rel}}(\ell)$ as

$$\mathcal{X}_h^{\text{rel}}(\ell) = \frac{\sum_{k=|\ell|}^{T/h-1-|\ell|} 1_{\{N_1(I_k^h) > 0, N_2(I_{k+\ell}^h) > 0\}}}{\min \left\{ \sum_{k=|\ell|}^{T/h-1-|\ell|} 1_{\{N_1(I_k^h) > 0\}}, \sum_{k=|\ell|}^{T/h-1-|\ell|} 1_{\{N_2(I_{k+\ell}^h) > 0\}} \right\}}.$$

Using this expression, we can relate $\mathcal{X}_h^{\text{rel}}(\ell)$ to the *cross-pair correlation function (CPCF)* of N .

To state the theoretical result formally, we introduce several assumptions and notation. We assume that $N = (N_1, N_2)$ is a simple stationary bivariate point process on \mathbb{R} with intensities $\lambda_1, \lambda_2 \in (0, \infty)$. Note that we use the term ‘‘intensity’’ in the same sense as in [23] (see page 47 *ibidem*). By [23, Proposition 3.3.IV], we have $\lambda_a = \mathbb{E}[N_a((0, 1])]$ for $a = 1, 2$. We also assume that there exists a locally integrable function $\lambda_{12} : \mathbb{R} \rightarrow [0, \infty]$ such that

$$\mathbb{E}[N_1(A_1)N_2(A_2)] = \int_{A_1 \times A_2} \lambda_{12}(y - x) dx dy \quad (3.1)$$

for any bounded $A_1, A_2 \in \mathcal{B}(\mathbb{R})$. We refer to λ_{12} as the *cross-intensity function*² of N . The CPCF of N is the function $g : \mathbb{R} \rightarrow [0, \infty]$ defined as

$$g(u) = \frac{\lambda_{12}(u)}{\lambda_1 \lambda_2} \quad (u \in \mathbb{R}).$$

The cross-intensity function can be related to the cross-covariance function between the infinitesimal increments of N_1 and N_2 in the following sense (cf. (A.11)):

$$\nu_{12}(u) := \lim_{h \downarrow 0} \frac{\text{Cov}(N_1(0, h], N_2(u, u + h])}{h^2} = \lambda_{12}(u) - \lambda_1 \lambda_2 \quad \text{a.e. } u.$$

The function ν_{12} is called the *covariance density* of N . In this sense, $g(u)$ measures the cross-covariation between $N_1(\cdot)$ and $N_2(\cdot + u)$.

We also need the notion of α -mixing (or strong mixing) for point processes. Recall that the α -mixing coefficient of two sub- σ -algebras \mathcal{G} and \mathcal{H} of \mathcal{F} is defined as

$$\alpha(\mathcal{G}, \mathcal{H}) := \sup \{ |\mathbb{P}(C \cap D) - \mathbb{P}(C)\mathbb{P}(D)| : C \in \mathcal{G}, D \in \mathcal{H} \}.$$

For $E \in \mathcal{B}(\mathbb{R})$, we denote by $N \cap E = (N_i \cap E)_{i=1}^2$ the restriction of N to E , i.e. $(N_i \cap E)(A) = N_i(A \cap E)$ for $i = 1, 2$ and $A \in \mathcal{B}(\mathbb{R})$. Also, $E \oplus r := \{x \in \mathbb{R} : |y - x| < r \text{ for some } y \in E\}$ denotes the r -enlargement of E . Moreover, given a bivariate point process $M = (M_1, M_2)$ on \mathbb{R} , $\sigma(M)$ denotes the σ -algebra generated by $\bigcup_{i=1}^2 \{M_i(A) : A \in \mathcal{B}(\mathbb{R})\}$. As α -mixing coefficients of N , we adopt the following definition:

$$\begin{aligned} \alpha_{c_1, c_2}^N(m; r) &= \sup \left\{ \alpha(\sigma(N \cap E_1), \sigma(N \cap E_2)) : E_1 = \bigcup_{j \in J_1} I_j \oplus r, E_2 = \bigcup_{j \in J_2} I_j \oplus r, \right. \\ &\quad \left. |J_1| \leq c_1, |J_2| \leq c_2, d(J_1, J_2) \geq m, J_1, J_2 \subset \mathbb{Z} \right\}, \quad m, c_1, c_2, r \geq 0, \end{aligned} \quad (3.2)$$

²In neuroscience, the term ‘‘cross-intensity function’’ usually refers to the functions $\lambda_{12}(u)/\lambda_1$ or $\lambda_{12}(u)/\lambda_2$ (see e.g. [15]). We follow the terminology used in spatial statistics [41, 42]. In the terminology of point process theory, λ_{12} is a density of the reduced cross-moment measure of N (cf. [23, Section 8.3]).

where $I_j := I_j^1 = (j, j+1]$ and $d(J_1, J_2) := \inf\{|j_1 - j_2| : j_1 \in J_1, j_2 \in J_2\}$. This definition is a minor variant of the one used in [65], where they use $(j - \frac{1}{2}, j + \frac{1}{2}]$ instead of I_j . This difference is inessential, and we just adopt the present definition to (slightly) simplify our technical arguments.

Remark 3.1 (Mixing coefficients as a continuous-time process). Since N can be regarded as a stochastic process indexed by \mathbb{R} , we can also define the α -mixing coefficients in this sense [14]:

$$\alpha_{\text{proc}}^N(\tau) := \sup_{t \in \mathbb{R}} \alpha(\sigma(N \cap (-\infty, t)), \sigma(N \cap (t + \tau, \infty))), \quad \tau \geq 0.$$

Our definition is weaker than this version in the sense that we have

$$\alpha_{c_1, c_2}^N(m; r) \leq \alpha_{\text{proc}}^N(m - 2r) \quad (3.3)$$

for all $c_1, c_2, r \geq 0$ and $m \geq 2r$. For the case of point processes, it is important to work with the weaker version because it is sometimes difficult to bound the left hand side of (3.3) uniformly in $c_1, c_2 \geq 0$; see [57, Proposition 2.8] and [65, Lemma 10.13] for example.

We impose the following regularity conditions on N .

- [A1] (i) For every $p \geq 1$, there exists a constant $B_p > 0$ such that $\max_{i=1,2} \lambda_i^{-1} \|N_i((0, 1])\|_p \leq B_p$.
- (ii) For any $p, q \geq 1$, there exists a constant $B_{p,q} > 0$ such that $\alpha_{p,p}^N(m; r_1) \leq B_{p,q} m^{-q}$ for all $m \in \mathbb{N}$, where $r_1 := r + 1$.

This assumption is fairly reasonable in the literature and is satisfied by many standard point process models such as the Hawkes process and Neyman-Scott process as long as their kernels satisfy some regularity conditions; see Section 5.1 for details.

Under [A1] and additional technical assumptions, we have the following asymptotic representation of Dobrev–Schaumburg’s cross-market activity measure:

Proposition 3.1. *Assume [A1]. Assume also that g is bounded and*

$$\begin{aligned} \max_{\ell \in \mathcal{G}_h} \mathbb{E}[N_1(I_0^h) \{N_1(I_0^h) - 1\} N_2(I_\ell^h)] &= o(h^{1+\varpi}), \\ \max_{\ell \in \mathcal{G}_h} \mathbb{E}[N_1(I_0^h) N_2(I_\ell^h) \{N_2(I_\ell^h) - 1\}] &= o(h^{1+\varpi}) \end{aligned} \quad (3.4)$$

as $h \rightarrow 0$ for $\varpi = 1$. Moreover, assume $h = h_T \asymp T^{-\gamma}$ as $T \rightarrow \infty$ for some $0 < \gamma < 1$. Then

$$\max_{\ell \in \mathcal{G}_h} \left| \frac{\mathcal{X}_h^{\text{rel}}(\ell)}{h} - (\lambda_1 \vee \lambda_2) \int_{\mathbb{R}} \frac{1}{h} K^{\text{tri}} \left(\frac{u - \ell h}{h} \right) g(u) du \right| \rightarrow^p 0,$$

where $K^{\text{tri}}(x) = (1 - |x|)1_{[-1,1]}(x)$.

Remark 3.2 (On condition (3.4)). The quantities on the left hand sides of (3.4) can be related to the factorial moment measures of orders (2,1) and (1,2) of N (see Section 2.3 of [65] for the definition). In particular, (3.4) holds for $\varpi = 1$ if these measures have bounded densities with respect to the Lebesgue measure. Since each factorial moment measure can be expressed as a sum of factorial cumulant measures through [65,

Eq.(2.5)] (see also [12, Eq.(3.21)]), its density can be computed for the Hawkes process via [48, Eq.(39)] and the Neyman-Scott process via [65, Eq.(5.2)], respectively; hence, one can in principle verify (3.4) under appropriate assumptions on their kernels. We do not pursue this point further because this condition is unnecessary for the theoretical development of our new estimator proposed in the next section.

Under the assumptions of Proposition 3.1, we have $\max_{\ell \in \mathcal{G}_h} |\mathcal{X}_h^{\text{rel}}(\ell)/h - (\lambda_1 \vee \lambda_2)g(\ell h)| \rightarrow^p 0$ if g is continuous. Hence, the cross-market activity measure can be interpreted as an estimator for the CPCF up to a multiplicative constant. Moreover, if g has a unique maximizer θ^* in $(-r, r)$, the above result implies that $\hat{\theta}_h^{DS}$ is a consistent estimator of θ^* as $T \rightarrow \infty$. For further understanding of theoretical properties of $\hat{\theta}_h^{DS}$, we study its rate of convergence. For this purpose, we introduce the following assumption on g :

[A2] There exist constants $\theta^* \in (-r, r)$, $\alpha \in (0, 1) \cup (1, \infty)$, $b > 1$ and $\delta > 0$ such that the following conditions hold:

(i) If $\alpha > 1$, $\sup_{u \in \mathbb{R}} g(u) \leq b$ and

$$\min \left\{ \sup_{0 < u - \theta^* < \delta} \frac{g(\theta^*) - g(u)}{|u - \theta^*|^{\alpha-1}}, \sup_{0 < \theta^* - u < \delta} \frac{g(\theta^*) - g(u)}{|u - \theta^*|^{\alpha-1}} \right\} \leq b$$

and

$$\inf_{0 < |u - \theta^*| < \delta} \frac{g(\theta^*) - g(u)}{|u - \theta^*|^{\alpha-1}} \geq \frac{1}{b}$$

and

$$\sup_{|u - \theta^*| \geq \delta} g(u) \leq g(\theta^*) - \frac{1}{b}.$$

(ii) If $\alpha < 1$,

$$\max \left\{ \inf_{0 < u - \theta^* < \delta} \frac{g(u)}{|u - \theta^*|^{\alpha-1}}, \inf_{-\delta < u - \theta^* < 0} \frac{g(u)}{|u - \theta^*|^{\alpha-1}} \right\} \geq \frac{1}{b}.$$

Moreover, there exist a constant $\alpha < \alpha_0 \leq 1$ and a measurable function $g_0 : \mathbb{R} \rightarrow [0, \infty]$ such that $\|g_0\|_{L^{1/(1-\alpha_0)}([-r_1, r_1])} \leq b$ and

$$g(u) \leq b(g_0(u) + |u - \theta^*|^{\alpha-1}) \quad \text{for all } u \in [-r_1, r_1].$$

Under [A2](i), g is bounded and θ^* is the unique maximizer of g . By contrast, under [A2](ii), g diverges at θ^* and is therefore unbounded. We allow g to have poles other than θ^* through an auxiliary function g_0 ; however, the condition $\|g_0\|_{L^{1/(1-\alpha_0)}([-r_1, r_1])} < \infty$ ensures that θ^* remains the “sharpest” peak location of g . We call θ^* the *lead-lag (time) parameter*. We allow g to be unbounded motivated by several empirical observations: (i) Dobrev–Schaumburg’s cross-market activity measure often exhibits extremely sharp peaks (see e.g. [27, Fig. 7]); (ii) Shiotani & Yoshida [65] found that their semiparametric model fits Japanese stock market data better when the CPCF is unbounded; (iii) Rambaldi *et al.* [60] report that intensity burst occurrences across different foreign exchange rates exhibit lead-lag relationships.

Remark 3.3 (Relation to mode estimation). Our formulation of the lead-lag parameter estimation problem is naturally connected to mode estimation for a probability density function, once the CPCF is replaced by the density. [A2] is motivated by this observation. In fact, Wegman [71] classifies the problem of mode

estimation for unimodal distributions into three types, labeling cases with bounded density as Type I, cases with unbounded density as Type II, and cases without density as Type III. In this classification, [A2](i) corresponds to Type I, and [A2](ii) corresponds to Type II. For the purpose of analyzing the convergence rate, we assume that the CPCF behaves like a power function $|u - \theta^*|^{\alpha-1}$ in a neighborhood of θ^* . When $\alpha > 1$, this assumption is analogous to the conditions studied in [3] (see Section 1.1 *ibidem*). When $\alpha < 1$, it corresponds to the analogue of condition **[H-III]** in [9]. Note that the case $\alpha = 1$ is excluded simply because the power function $|u - \theta^*|^{\alpha-1}$ becomes constant in that case.

Under [A2], we set

$$\beta_\alpha := \alpha \vee (2\alpha - 1) = \begin{cases} \alpha & \text{if } \alpha < 1, \\ 2\alpha - 1 & \text{if } \alpha > 1. \end{cases}$$

Theorem 3.1. *Assume [A1], [A2] and $h = h_T \asymp T^{-\gamma}$ as $T \rightarrow \infty$ for some $0 < \gamma < 1/\beta_\alpha$. Moreover, assume (3.4) for $\varpi = \alpha$. Then, $\hat{\theta}_h^{DS} = \theta^* + O_p(h)$ as $T \rightarrow \infty$.*

Since $\hat{\theta}_h^{DS}$ is, by construction, an integer multiple of h , Theorem 3.1 implies that its convergence rate is exactly of order $O(h)$. In particular, the accuracy of $\hat{\theta}_h^{DS}$ improves as h becomes smaller. Given the definition of $\mathcal{X}_h^{\text{rel}}(\ell)$, however, it is meaningless to choose h smaller than the minimum time unit in the data. In this sense, it is reasonable that Dobrev & Schaumburg [27] set h equal to the minimum time resolution.

Nevertheless, Theorem 3.1 also imposes a constraint on the order of h , requiring that h converge to 0 more slowly than T^{-1/β_α} . Moreover, this constraint is not a technical artifact of the proof; it is essential, because we show that T^{-1/β_α} gives a minimax lower bound on the convergence rate of any estimator of θ^* under the assumptions of Theorem 3.1, at least when $\alpha < 2$ (see Remark 4.2). Therefore, it is theoretically impossible for the conclusion of Theorem 3.1 to hold when $h \ll T^{-1/\beta_\alpha}$.

Note that $n_a/T \rightarrow \lambda_a > 0$ as $T \rightarrow \infty$ a.s. for each $a = 1, 2$ under [A1]. Hence, for $\hat{\theta}_h^{DS}$ to perform properly, h must be chosen based on n_1, n_2 (the sample sizes) and α (the sharpness of the CPCF peak). Specifically, h should be taken larger when n_1 and n_2 are smaller and/or when α is larger. This provides one explanation for the poor performance of the Dobrev–Schaumburg method in the example shown in Fig. 1. That is, in that dataset, setting $h = 1 \mu\text{s}$ was likely far too small, given the relatively small numbers of observations $(n_1, n_2) = (28048, 11287)$.

These observations indicate that the choice of h plays a crucial role in the implementation of the DS estimator. However, the DS estimator should be interpreted as an estimator of an interval containing the lead-lag parameter, rather than the parameter itself, which makes data-driven selection of h difficult. For these reasons, in the next section, we propose a new lead-lag time estimator based on kernel density estimation and demonstrate that it can overcome this issue.

4 New estimator

Proposition 3.1 suggests that $\mathcal{X}_h^{\text{rel}}(\ell)$ would be asymptotically equivalent to a discretized version of a kernel density estimator for g based on the triangular kernel. This naturally motivates us to consider kernel density estimators for g directly.

Formally, let $K : \mathbb{R} \rightarrow \mathbb{R}$ be a kernel function and $h = h_T > 0$ a bandwidth parameter such that $h \rightarrow 0$ as $T \rightarrow \infty$. We then consider the following statistic:

$$\hat{g}_h(u) = \frac{T}{n_1 n_2} \int_{(0,T]^2} K_h(y - x - u) N_1(dx) N_2(dy), \quad u \in \mathbb{R},$$

where $K_h(t) = h^{-1}K(t/h)$ for $t \in \mathbb{R}$. We estimate θ^* by taking a maximizer of \hat{g}_h . That is, we define a random variable $\hat{\theta}_h$ satisfying

$$\hat{\theta}_h \in \arg \max_{u \in [-r,r]} \hat{g}_h(u).$$

The practical procedure for computing $\hat{\theta}_h$ and its computational complexity are described in Appendix B.

When the uniform kernel is used as the kernel function, \hat{g}_h is essentially equivalent to the so-called *cross-correlation histogram* in neuroscience and has long been applied to investigate relationships between neuronal spikes (see e.g. [15]). This line of work has motivated statisticians to investigate the theoretical properties of \hat{g}_h [13, 14, 20, 32]. Nevertheless, to the best of our knowledge, no prior research has addressed the case where g is unbounded, nor the asymptotic behavior of the maximizer of \hat{g}_h .

We impose the following assumption on the kernel.

[K] K is non-negative, continuous at 0, of bounded variation and supported on $[-1, 1]$ such that $K(0) > 0$, $\int_{-\infty}^{\infty} K(t)dt = 1$ and $\arg \max_{u \in [-r,r]} \hat{g}_h(u) \neq \emptyset$ a.s.

Assumption [K] holds for the uniform kernel $K = \frac{1}{2}1_{[-1,1]}$ and the triangular kernel $K = K^{\text{tri}}$, for example.

Theorem 4.1. *Assume [A1], [A2] and [K]. Let $\eta > 0$ be a constant. Then, there exist constants $A > 1$ and $0 < h_0 < 1$ depending only on $\alpha, \alpha_0, \delta, b$ and K such that*

$$\mathbb{P}(|\hat{\theta}_h - \theta^*| > Ah) \leq \frac{C}{\sqrt{Th^{\beta_\alpha + \varepsilon}}} \quad (4.1)$$

for all $h \leq h_0 \wedge T^{-\eta}$ and $\varepsilon > 0$, where $C > 0$ is a constant depending only on $r, \alpha, \delta, b, (B_p)_{p \geq 1}, (B_{p,q})_{p,q \geq 1}, \varepsilon, \eta$ and $\|K\|_\infty$. In particular, $\hat{\theta}_h = \theta^* + O_p(h)$ as $T \rightarrow \infty$ if $h = h_T \asymp T^{-\gamma}$ for some $0 < \gamma < 1/\beta_\alpha$.

By Theorem 4.1, $\hat{\theta}_h$ estimates θ^* at the same convergence rate as $\hat{\theta}_h^{\text{DS}}$. Moreover, unlike the DS estimator, we do not require assumption (3.4). In particular, by selecting the bandwidth appropriately, our estimator nearly attains the minimax optimal convergence rate T^{-1/β_α} (see Theorem 4.3). The next subsection discusses methods for selecting the bandwidth in a data-driven way.

Remark 4.1 (Relation to kernel mode estimation). In light of Remark 3.3, our estimator is closely related to a mode estimator obtained by maximizing a kernel density estimator. Following [17], we refer to this type of estimator as the kernel mode estimator.

For i.i.d. data with density f and unique population mode θ^* , Parzen [55] established the asymptotic normality of the kernel mode estimator when f is of class C^2 and $f''(\theta^*) < 0$. This setting is a particular case of [A2] with $\alpha = 3$. Notably, with a suitable bandwidth choice, the kernel mode estimator nearly achieves the convergence rate $n^{-1/5}$, where n is the sample size. Since $\beta_3 = 5$, our estimator enjoys an

analogous property. Has'minskii [36] proved that the rate $n^{-1/5}$ is minimax optimal in this setting, but it can be improved under additional smoothness assumptions on the density and the kernel; see e.g. [31, 49, 70].

Without smoothness assumptions on the density, Abraham *et al.* [1] and Herrmann & Ziegler [40] obtained convergence rates for the kernel mode estimator and its variant under conditions analogous to [A2](i). In this scenario, Arias-Castro *et al.* [3] established the minimax optimal rate and developed an adaptive estimation procedure. The convergence rate in this setting is $n^{-1/(2\alpha-1)}$, which again analogous to ours. To the best of our knowledge, apart from the work of [9], no results exist for mode estimation under assumptions analogous to [A2](ii). Bercu *et al.* [9] investigated a histogram-type estimator, which can be viewed as a discretized kernel mode estimator, and showed that its convergence rate can be made arbitrarily close to $n^{-1/\alpha}$ by selecting the bin width appropriately. This behavior is also analogous to that of our estimator.

Finally, to our knowledge, the asymptotic distribution of the kernel mode estimator remains unknown for non-smooth densities. We conjecture that it may be non-Gaussian when $\alpha < 3/2$, drawing a parallel to location parameter estimation in the presence of density singularities (cf. [46, Chapter VI]).

4.1 Bandwidth selection by Lepski's method

In the classical setting of i.i.d. observations and kernel density estimation, bandwidth selection is typically based on minimizing the mean integrated squared error (MISE) of the kernel estimator; see, for example, [69, Chapter 1]. In kernel estimation of moment density functions for point processes, analogous MISE-type criteria are also standard [34, 47].

However, for our purposes, a global loss criterion such as MISE is not entirely satisfactory, because the object of interest is not the function g itself but the location θ^* of its peak. Intuitively, a global criterion aims to fit the entire curve, including regions where g is only moderately large or small, whereas the estimation error of θ^* may be governed almost exclusively by the local behaviour of g in a small neighbourhood of the peak, which may even be singular under condition [A2](ii). A closely related issue has been recognized in the literature on nonparametric modal regression with i.i.d. observation; see, for example, Section 4.2 in Chen [18]. Motivated by recent works in this context [19, 72], we investigate loss-minimization approaches based on cross-validation in Appendix C.

Here, we instead adopt an adaptive estimation strategy based on a Lepski-type method, i.e., a pairwise comparison of estimators with different bandwidths. Our approach was particularly inspired by Klemelä [49], who has developed a Lepski-type method for mode estimation from i.i.d. data. For textbook treatments of Lepski's method, we refer to [33, Section 8.2].

Fix constants $a > 1$, $\gamma_{\max} > 0$ and $j_{\min} \in \mathbb{N}$. We consider the following set as candidates for bandwidths:

$$\mathcal{H}_T := \{a^{-j} : j_{\min} \leq j \leq \lceil \log_a(T^{\gamma_{\max}}) \rceil, j \in \mathbb{Z}\}.$$

For every $h \in \mathcal{H}_T$, set

$$\mathcal{M}_h := \arg \max_{u \in [-r, r]} \hat{g}_h(u).$$

We define

$$\hat{h} := \min \{h \in \mathcal{H}_T : \bar{d}(\mathcal{M}_h, \mathcal{M}_{h'}) \leq A_T h' \text{ for all } h' \in \mathcal{H}_T \text{ with } h' \geq h\},$$

where A_T is a positive constant and

$$\bar{d}(\mathcal{M}_h, \mathcal{M}_{h'}) := \sup \{ |x - y| : x \in \mathcal{M}_h, y \in \mathcal{M}_{h'} \}.$$

Theorem 4.2. *Assume [A1], [A2] and [K]. Also, assume $1/\beta_\alpha \leq \gamma_{\max}$. Further, assume $A_T \rightarrow \infty$ and $A_T = o(T^c)$ for any $c > 0$ as $T \rightarrow \infty$. Then, $\hat{\theta}_{\hat{h}} = \theta^* + O_p(T^{-\gamma})$ for any $0 < \gamma < 1/\beta_\alpha$.*

Theorem 4.2 shows that the estimator $\hat{\theta}_{\hat{h}}$ nearly achieves the optimal convergence rate T^{-1/β_α} without requiring the precise value of α . This result is numerically validated in Section 5.3, where we also assess the robustness of the estimator with respect to the choice of the tuning parameter A_T . We will see that setting A_T to a constant multiple of $\log \log T$ performs reasonably well.

4.2 Minimax lower bound for the convergence rate

In this subsection, we show that when [A1] and [A2] hold, T^{-1/β_α} gives a minimax lower bound for the convergence rate of any estimator for θ^* . For this purpose, we consider a subclass of models for N satisfying [A1] and [A2], which is specified as follows. Given a probability density function g on \mathbb{R} , we consider a probability measure P_g on (Ω, \mathcal{F}) having the following properties:

- (i) $N_1 = \sum_{i=1}^{\infty} \delta_{t_i}$ is a Poisson process on \mathbb{R} with unit intensity under P_g .
- (ii) N_2 is of the form $N_2 = \sum_{i=1}^{\infty} \delta_{t_i + \gamma_i}$, where $(\gamma_i)_{i=1}^{\infty}$ is a sequence of i.i.d. random variables independent of N_1 such that the law of γ_1 has density g under P_g .

Under P_g , N is a bivariate Poisson process on \mathbb{R} in the sense of [23, Example 6.3(e)], where we have $Q_1 = Q_2 = 0$ and $Q_3(dx dy) = g(y - x) dx dy$ in their notation. In particular, under P_g , the CPCF of N is given by g .

We write $\mathcal{G}(\theta^*, \alpha, \delta, b)$ for the class of probability density functions $g : \mathbb{R} \rightarrow [0, \infty]$ supported on $[-1, 1]$ and satisfying the conditions of [A2]. Note that if $g \in \mathcal{G}(\theta^*, \alpha, \delta, b)$, then N satisfies [A1] and [A2] for some family of constants $(B_p)_{p \geq 1}$. In fact, [A2] is evident, while [A1](i) follows from the fact that both N_1 and N_2 are Poisson processes on \mathbb{R} with unit intensity. Finally, since g is supported on $[-1, 1]$, $\alpha_{c_1, c_2}^N(m; r_1) = 0$ for $m \geq m_0$, where m_0 depends only on r . Hence, [A1](ii) is also satisfied. Given this consideration, the following theorem shows that T^{-1/β_α} gives a minimax lower bound for the convergence rate of any estimator for θ^* under [A1] and [A2]:

Theorem 4.3. *For any $\alpha \in (0, 1) \cup (1, \infty)$, there exists a constant $b > 0$ such that*

$$\liminf_{T \rightarrow \infty} \inf_{\hat{\theta}_T} \sup_{|\theta| \leq 2\rho_T} \sup_{g \in \mathcal{G}(\theta, \alpha, 1/2, b)} P_g \left(|\hat{\theta}_T - \theta| \geq \rho_T \right) > 0,$$

where $\rho_T := T^{-1/\beta_\alpha}$ and the infimum is taken over all estimators based on $N \cap [0, T]$, i.e. all $\sigma(N \cap [0, T])$ -measurable random variables.

Remark 4.2. Since the cumulant measure of order (p, q) of N vanishes if $p \wedge q > 1$, condition (3.4) holds whenever $\varpi = 1$, and also holds for $\varpi < 2$ when g is bounded. Therefore, T^{-1/β_α} is also a minimax lower bound for the convergence rate of any estimator for θ^* under the assumptions of Theorem 3.1 when $\alpha < 2$.

5 Simulation study

Bivariate Hawkes and Neyman–Scott processes equipped with gamma kernels are used to model the relationship between two series of timestamps in high-frequency financial data; for instance, see [58] and [65], respectively. In our experiments, we employ “lagged” variants of these models as the data-generating processes. Using simulated data, we numerically investigate the accuracy, convergence rate, and tuning parameter sensitivity of the DS estimator and our proposed estimator. We adopt the triangular kernel K_{tri} for the kernel method in all numerical experiments in this paper.

5.1 Models

5.1.1 Lagged bivariate Hawkes process with gamma kernels

First, we introduce a bivariate Hawkes process with conditional intensity functions

$$\lambda_i(t) = \mu_i + \sum_{t_{k,1} < t} \phi_{i1}(t - t_{k,1}) + \sum_{t_{k,2} < t} \phi_{i2}(t - t_{k,2}), \quad i = 1, 2,$$

where $\{t_{k,i}\}$ denotes the k -th event time in the i -th component. We parameterize the kernel functions as $\phi_{ij}(t) = \alpha_{ij} h_{ij}(t)$ for $t > 0$, where $\alpha_{ij} > 0$ is the branching ratio and $h_{ij}(t)$ is a probability density function on $(0, \infty)$.

In this study, we adopt gamma kernels. Specifically, we assume that h_{ij} follows a gamma density $\Gamma(D_{ij}, \beta_{ij})$:

$$h_{ij}(t) = \frac{\beta_{ij}^{D_{ij}}}{\Gamma(D_{ij})} t^{D_{ij}-1} e^{-\beta_{ij}t}, \quad t > 0,$$

where $D_{ij} > 0$ is the shape parameter and $\beta_{ij} > 0$ is the rate parameter. When $D_{ij} = 1$, this specification reduces to the classical exponential kernel, so the exponential Hawkes model is included as a special case. We write $\boldsymbol{\mu} = (\mu_1, \mu_2)^\top$ for the baseline intensity vector, and $\boldsymbol{\alpha} = (\alpha_{ij})_{1 \leq i, j \leq 2}$, $\boldsymbol{\beta} = (\beta_{ij})_{1 \leq i, j \leq 2}$, and $\boldsymbol{D} = (D_{ij})_{1 \leq i, j \leq 2}$ for the matrices of branching ratios, rate parameters, and shape parameters, respectively. We then collect all kernel and baseline parameters into

$$\eta = (\boldsymbol{\mu}, \boldsymbol{\alpha}, \boldsymbol{\beta}, \boldsymbol{D}) \in (0, \infty)^2 \times (0, \infty)^{2 \times 2} \times (0, \infty)^{2 \times 2} \times (0, \infty)^{2 \times 2}.$$

We assume the spectral radius of $\boldsymbol{\alpha}$ is smaller than 1 to ensure stationarity. Following Bacry *et al.* [4], the intensity is

$$\Lambda = (\lambda_1(\eta), \lambda_2(\eta))^\top = (I_2 - \boldsymbol{\alpha})^{-1} \boldsymbol{\mu}$$

(Eq.(3) in [4]), and the CPCF is

$$g(u; \eta, \theta) = 1 + \frac{\nu_{12}(u; \eta)}{\lambda_1(\eta) \lambda_2(\eta)}, \quad u \in \mathbb{R},$$

where ν_{12} is the (1, 2) component of the infinitesimal covariance matrix ν of the bivariate Hawkes process (Eq.(8) in [4]):

$$\nu_{12}(u) = \left(\Psi(u) \Sigma + \Sigma \Psi^\top(-u) + \tilde{\Psi} * \Sigma \Psi^\top(u) \right)_{1,2} \quad u \in \mathbb{R}, \quad (5.1)$$

where $\Sigma = \text{diag}\{\lambda_1, \lambda_2\}$, $\Psi(u) = (\Psi_{ij}(u))_{1 \leq i, j \leq 2}$ is defined by

$$\Psi(u) = \sum_{m=1}^{\infty} \Phi^{(*m)}(u), \quad \Phi^{(*m)} = \underbrace{\Phi * \cdots * \Phi}_{m \text{ times}},$$

with kernel matrix $\Phi(u) = (\phi_{ij}(u))_{1 \leq i, j \leq 2}$ and $*$ denoting the matrix convolution, and $\tilde{\Psi}(u) = \Psi(-u)$, $u \in \mathbb{R}$.

In addition, let $\theta \in \mathbb{R}$ denote the lead-lag parameter. Given a realization of the bivariate Hawkes process $N = (N_1^0, N_2^0)$, we call the shifted process $(N_1, N_2) = (N_1^0, N_2^0(\cdot - \theta))$ a *lagged bivariate Hawkes process with gamma kernels (LBHPG)*. Its distribution is denoted by

$$\text{LBHPG}(\eta, \theta).$$

For the shifted process $\text{LBHPG}(\eta, \theta)$, the intensity is still Λ , while the cross-covariance density is simply shifted:

$$\nu_{12}(u - \theta; \eta), \quad u \in \mathbb{R}.$$

Also, we have the cross-pair correlation function (CPCF) of $\text{LBHPG}(\eta, \theta)$ as

$$g(u; \eta, \theta) = 1 + \frac{\nu_{12}(u - \theta; \eta)}{\lambda_1(\eta) \lambda_2(\eta)}, \quad u \in \mathbb{R}. \quad (5.2)$$

In the simulation study, we restrict to the case of common rate parameters, that is, $\beta_{ij} \equiv \beta$ for all $i, j \in \{1, 2\}$. In such cases, $\text{LBHPG}(\eta, \theta)$ satisfies [A2](ii) with $\alpha = \min\{D_{12}, D_{21}\}$ if $\min\{D_{12}, D_{21}\} < 1$ (diverging gamma kernel(s)) and [A2](i) with $\alpha = 2$ if $D_{11} = D_{21} = D_{12} = D_{22} = 1$ (exponential kernels). The former can be obtained by the reproducibility of gamma densities and the local behavior of bilateral gamma densities at the origin [51, Thm. 6.1]. For details, see Appendix A.7. The latter follows from the explicit formula for the CPCF for bivariate Hawkes processes with exponential kernels, which can be obtained by [6, Example 3]. The moment condition [A1](i) is guaranteed thanks to Theorem 1 in [52]. We also have a bound on the strong mixing rate [A1](ii) from Theorem 3.1 in [11], since the gamma kernels decay geometrically. Therefore, $\text{LBHPG}(\eta, \theta)$ satisfies the assumptions in Theorem 4.1 with a (smoothing) kernel satisfying Assumption [K] in such special cases.

5.1.2 Lagged bivariate Neyman-Scott process with gamma kernels

First, we recall the construction of a bivariate Neyman-Scott process on \mathbb{R} following Section 5.1 in Shiotani & Yoshida [65]. Let \mathcal{C} be a homogeneous Poisson (parent) process on \mathbb{R} with intensity $\lambda > 0$. For $i = 1, 2$ and each $c \in \mathcal{C}$, let $M_i(c)$ be the number of offspring in the component i from the parent c . We assume that $\{M_i(c)\}_{c \in \mathcal{C}}$ are i.i.d. copies of a $\mathbb{Z}_{\geq 0}$ -valued random variable M_i with finite mean $\sigma_i = \mathbb{E}[M_i] \in (0, \infty)$, $i = 1, 2$. For simplicity, we assume that M_i follows a Poisson distribution $\text{Poi}(\sigma_i)$, $i = 1, 2$. Conditional on $M_i(c)$, the temporal offsets $\{d_i(c, m)\}_{m=1}^{M_i(c)}$ of the offspring are i.i.d. with density f_i , independent over i, c, m and independent of \mathcal{C} and $\{M_i(c)\}$. Then, let

$$N_i^0 = \sum_{c \in \mathcal{C}} \sum_{m=1}^{M_i(c)} \delta_{c+d_i(c, m)}, \quad i = 1, 2.$$

We call $N^0 = (N_1^0, N_2^0)$ a bivariate Neyman-Scott process.

N^0 is stationary with intensities

$$\lambda_i(\xi) = \lambda \sigma_i, \quad i = 1, 2.$$

Moreover, the cross-intensity of (N_1^0, N_2^0) is

$$\lambda_{12}(u; \xi) = \lambda^2 \sigma_1 \sigma_2 + \lambda \sigma_1 \sigma_2 \int_{\mathbb{R}} f_1(s; \tau_1) f_2(u + s; \tau_2) ds, \quad u \in \mathbb{R},$$

see Eq.(5.2) and the subsequent calculation in [65]. Therefore, the cross-pair correlation function (CPCF) of the bivariate Neyman-Scott process is

$$g(u; \xi) = \frac{\lambda_{12}(u; \xi)}{\lambda_1(\xi) \lambda_2(\xi)} = 1 + \frac{1}{\lambda} \int_{\mathbb{R}} f_1(s; \tau_1) f_2(u + s; \tau_2) ds, \quad u \in \mathbb{R},$$

where ξ collects all parameters introduced above.

In this simulation study, we adopt gamma dispersal kernels as in the NBNSP-G model of Shiotani and Yoshida [65]. Specifically, for $i = 1, 2$ we assume that

$$f_i(u; \tau_i) = \frac{l_i^{\alpha_i}}{\Gamma(\alpha_i)} u^{\alpha_i-1} e^{-l_i u} 1_{(0, \infty)}(u), \quad u \in \mathbb{R},$$

where $\tau_i = (\alpha_i, l_i)$, $\alpha_i > 0$ is the shape parameter and $l_i > 0$ is the rate parameter of the gamma law. We then collect the parameters as

$$\xi = (\lambda, \sigma_1, \sigma_2, \alpha_1, \alpha_2, l_1, l_2) \in (0, \infty)^7.$$

Let $\theta \in \mathbb{R}$ denote the lead-lag parameter. Given a realization $N^0 = (N_1^0, N_2^0)$ of the bivariate Neyman-Scott process with gamma kernels described above, we define the lagged process by shifting the second component:

$$(N_1, N_2) = (N_1^0, N_2^0(\cdot - \theta)).$$

We refer to $N = (N_1, N_2)$ as the *lagged bivariate Neyman-Scott process with gamma kernels (LBNSPG)* and denote its distribution by

$$\text{LBNSPG}(\xi, \theta).$$

The intensities of $\text{LBNSPG}(\xi, \theta)$ are still given by $\lambda_1(\xi)$ and $\lambda_2(\xi)$, while the cross-intensity is simply shifted:

$$\lambda_{12}(u - \theta; \xi), \quad u \in \mathbb{R}.$$

Consequently, the CPCF of $\text{LBNSPG}(\xi, \theta)$ is

$$\begin{aligned} g(u; \xi, \theta) &= \frac{\lambda_{12}(u - \theta; \xi)}{\lambda_1(\xi) \lambda_2(\xi)} = 1 + \frac{1}{\lambda} p(u - \theta; \tau_1, \tau_2), \\ p(u; \tau_1, \tau_2) &= \int_{\mathbb{R}} f_1(s; \tau_1) f_2(u + s; \tau_2) ds, \quad u \in \mathbb{R}. \end{aligned}$$

Name	Family	α	β_α	The convergence rate T^{-1/β_α}
<code>hawkes_gamma_sym</code>	LBHPG	0.4	0.4	$T^{-5/2}$
<code>hawkes_gamma_asym</code>	LBHPG	0.4	0.4	$T^{-5/2}$
<code>hawkes_exp</code>	LBHPG	2	3	$T^{-1/2}$
<code>ns_gamma_1</code>	LBNSPG	0.8	0.8	$T^{-5/4}$
<code>ns_gamma_2</code>	LBNSPG	1.6	2.2	$T^{-5/11}$
<code>ns_gamma_3</code>	LBNSPG	3	5	$T^{-1/5}$

Table 1: Values of α (the ‘‘sharpness’’ parameter of the CPCF g in [A2]; smaller values imply sharper functions), $\beta_\alpha = \alpha \vee (2\alpha - 1)$, and the minimax lower bound on the convergence rate T^{-1/β_α} in Theorem 4.3 for each model.

The function $p(\cdot; \alpha_1, \alpha_2, l_1, l_2)$ is the density of a bilateral gamma distribution. Küchler and Tappe [51] provide a detailed analysis of the shapes of bilateral gamma densities, including unimodality and the local behavior near zero (see Theorem 6.1 therein). Combining their results with the above representation shows that $g(\cdot; \xi, \theta)$ is strictly unimodal with the peak at θ whenever the parameters are symmetric, i.e., $\alpha_1 = \alpha_2$ and $l_1 = l_2$. We restrict attention to such symmetric cases in our simulation experiments. Under this restriction, LBNSPG(ξ, θ) satisfies [A2](ii) if $\alpha_1 + \alpha_2 < 1$ and [A2](i) if $\alpha_1 + \alpha_2 > 1$, with $\alpha = \min\{\alpha_1 + \alpha_2, 3\}$ in both cases.

Note that LBNSPG($\xi, 0$) is the special case (setting the noise process to zero and the distribution of M_i to Poisson) of the NBNSP-G model introduced in Section 6.1 in [65]. Therefore, LBNSPG($\xi, 0$) satisfies condition [NS] in [65], so that Lemma 10.13 there bounds the α -mixing coefficients of LBNSPG(ξ, θ) in terms of the tail probabilities of the dispersal kernels: for all $c_1 \geq 0$ and $m \geq 2r + 2$,

$$\alpha_{c_1, \infty}^N(m; r) := \sup_{c_2 \geq 0} \alpha_{c_1, c_2}^N(m; r) \leq 8m\lambda (m + 1 + 2r) \sum_{i=1}^2 \sigma_i \int_{|z| \geq m/2 - 2r} f_i(z; \tau_i) dz.$$

Since the gamma kernels have geometrically decaying tails, this implies that $\alpha_{c_1, \infty}(m; r_1)$ decreases faster than any power of m , so Assumption [A1](ii) holds for LBNSPG(ξ, θ). Moreover, since the Poisson-distributed M_i possesses moments of all orders, Lemma 10.14 in [65] yields finiteness of moments of $N_i((0, 1])$ of all orders, so that Assumption [A1](i) is satisfied. Therefore, LBNSPG(ξ, θ) fulfills Assumptions [A2] and [A1] and thus is in the scope of Theorem 4.1 if $\alpha_1 = \alpha_2$, $l_1 = l_2$, and $\alpha_1 + \alpha_2 \neq 1$.

5.1.3 Model and parameter specifications in the simulation studies

We consider two types of bivariate stationary point process models, each with three sets of parameter values. The models are labeled as `hawkes_gamma_sym`, `hawkes_gamma_asym`, `hawkes_exp`, `ns_gamma_1`, `ns_gamma_2`, and `ns_gamma_3`.

All LBHPG models share

$$\boldsymbol{\mu} = (0.2, 0.2)^\top, \quad \boldsymbol{\alpha} = \begin{pmatrix} 0.1 & 0.1 \\ 0.1 & 0.1 \end{pmatrix}, \quad \boldsymbol{\beta} = \begin{pmatrix} 10 & 10 \\ 10 & 10 \end{pmatrix}.$$

We use three specifications for the shape matrix \mathbf{D} to cover different degrees of regularity and asymmetry:

$$\begin{aligned}\text{hawkes_gamma_sym} : \quad \mathbf{D} &= \begin{pmatrix} 0.4 & 0.4 \\ 0.4 & 0.4 \end{pmatrix}; \\ \text{hawkes_gamma_asym} : \quad \mathbf{D} &= \begin{pmatrix} 0.4 & 0.4 \\ 0.8 & 0.4 \end{pmatrix}; \\ \text{hawkes_exp} : \quad \mathbf{D} &= \begin{pmatrix} 1 & 1 \\ 1 & 1 \end{pmatrix}.\end{aligned}$$

For the LBNSPG models, we fix

$$\lambda = 0.1, \quad \sigma_1 = \sigma_2 = 4$$

and use symmetric dispersal shape and rate parameters. We select three settings to vary the smoothness of the CPCF around the peak:

$$\begin{aligned}\text{ns_gamma_1} : \quad (\alpha_1, \alpha_2) &= (0.4, 0.4), \quad (l_1, l_2) = (10, 10), \\ \text{ns_gamma_2} : \quad (\alpha_1, \alpha_2) &= (0.8, 0.8), \quad (l_1, l_2) = (10, 10), \\ \text{ns_gamma_3} : \quad (\alpha_1, \alpha_2) &= (2.0, 2.0), \quad (l_1, l_2) = (100, 100).\end{aligned}$$

5.2 Accuracy

In this experiment, we compare the accuracy of the lead-lag time estimators using the root mean squared error (RMSE) across the six scenarios.

For each pair of observation time interval length $T \in \{1000, 2000, 4000, 8000\}$ and the estimator, we generate 5000 Monte Carlo replicates of sample paths. In every replicate, the true lead-lag time is drawn as $\theta^* \sim \mathcal{U}(-0.1, 0.1)$. For a given estimator $\hat{\theta}$, we report

$$\text{RMSE} = \left(\frac{1}{5000} \sum_{b=1}^{5000} (\hat{\theta}^{(b)} - \theta^{*(b)})^2 \right)^{1/2},$$

where $\hat{\theta}^{(b)}$ and $\theta^{*(b)}$ denote the estimate and the true lead-lag time in replicate b . Randomizing θ^* across replicates summarizes performance averaged over a range of lead-lag values rather than at a single fixed θ^* . The lead-lag time parameter is supposed to be in $(-1, 1)$, i.e., we set $r = 1$. The bandwidth grid is $\{10^{-1}, 10^{-2}, 10^{-3}, 10^{-4}, 10^{-5}, 10^{-6}\}$ for both the Lepski method and DS estimators. For the Lepski method, we set $A_T = \log \log T$. When the contrast function has multiple maximizers on $(-r, r)$, we select the minimum as a deterministic tie-breaking rule.

Figure 2 illustrates two systematic patterns. First, the performance of the DS estimator is sensitive to the bucket width h . For each T , the RMSE curves as a function of h are typically U-shaped: small buckets lead to high variance due to the scarcity of joint activations, whereas larger buckets introduce a discretization bias because the lead-lag time is constrained to a coarse grid. Moreover, the value of h that minimizes the RMSE

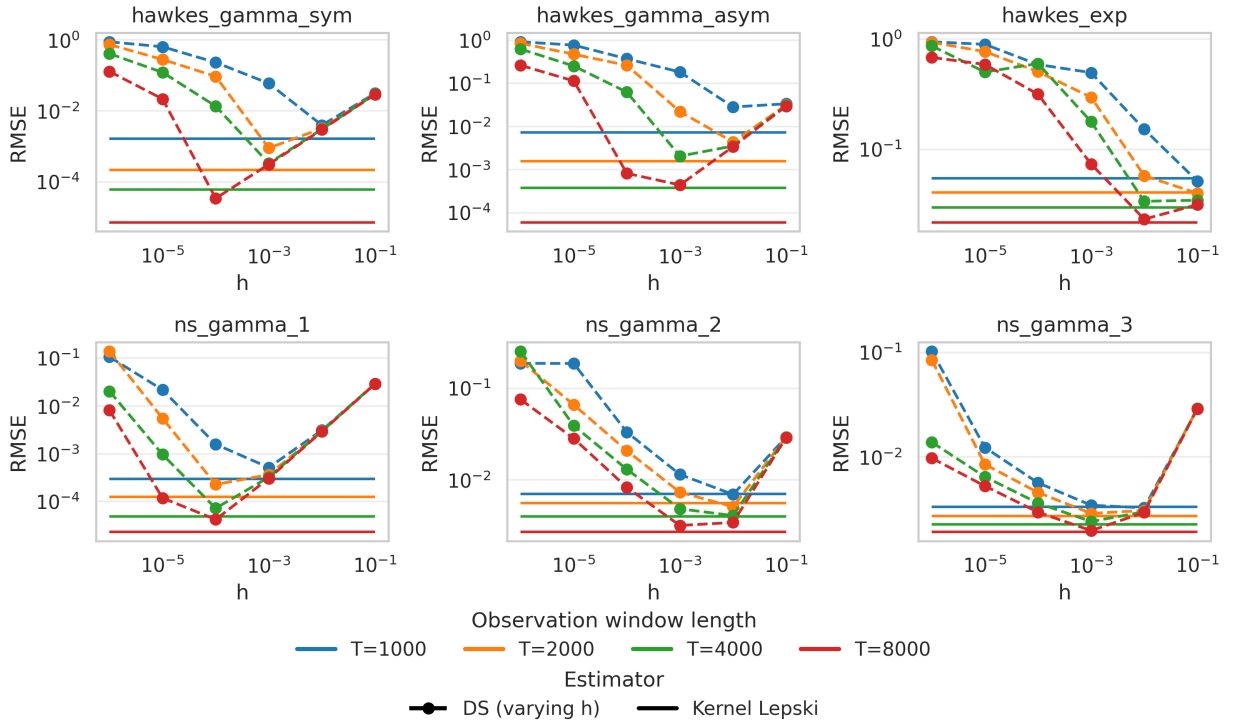


Figure 2: RMSE of the estimators for the lead-lag time across six scenarios. Each panel uses log–log axes with bandwidth h on the x-axis and RMSE on the y-axis. Dashed lines with markers trace the DS estimator over the bandwidth grid, while solid horizontal lines show the kernel estimator with the Lepski-selected bandwidth. Colors indicate the observation-window length $T \in \{1000, 2000, 4000, 8000\}$ and are shared across panels.

depends on both the underlying model and the observation window length T . This confirms that, in practice, the DS estimator requires model-specific tuning of h .

Second, the kernel estimator with Lepski’s bandwidth selection achieves lower RMSE than the DS estimator for almost all combinations of T and data-generating process. In Figure 2, the horizontal solid lines corresponding to the Lepski estimator lie close to (and often below) the best DS RMSE over the grid in each panel. Importantly, this improvement is obtained without any manual tuning of the bandwidth: once the grid \mathcal{H}_T and the slowly diverging constant $A_T = \log \log T$ are fixed, the procedure automatically adapts the smoothing level to the data. This demonstrates the main practical advantage of the proposed approach over the DS method.

5.3 Convergence rate and dependence on hyperparameters of Lepski’s method

In this experiment, we investigate the convergence rate of the Lepski estimator, as shown in Theorem 4.2. We also examine how the estimator behaves as the tuning parameter A_T varies.

As in the previous experiment, for each observation-window length $T \in \{1000, 2000, 4000, 8000\}$ and each estimator, we generate 5000 Monte Carlo replicates of sample paths. In every replicate, the true lead-lag time is drawn as $\theta^* \sim \mathcal{U}(-0.1, 0.1)$. The lead-lag time parameter is supposed to be in $(-1, 1)$, i.e., we set

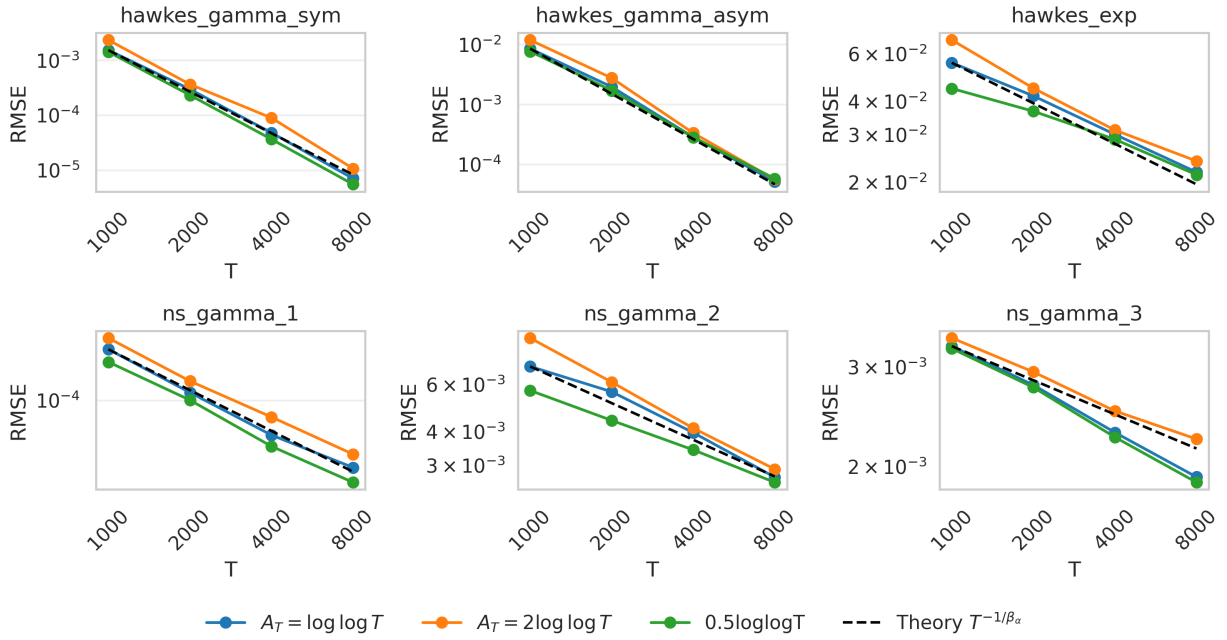


Figure 3: RMSE versus observation window T (log–log scale) across all simulation settings and A_T schedules. Theoretical T^{-1/β_α} slopes are shown as dashed lines.

$r = 1$. The bandwidth grid is $\{10^{-1}, 10^{-2}, 10^{-3}, 10^{-4}, 10^{-5}, 10^{-6}\}$.

Figure 3 investigates the convergence rate of the Lepski estimator. In each scenario, the RMSE is plotted against T on a log–log scale together with the theoretical slope T^{-1/β_α} derived from the minimax lower bound in Theorem 4.3. Across all six models, the empirical curves for the Lepski estimator are nearly parallel to the guideline. Thus, the proposed estimator may attain the optimal convergence rate given by our theory.

The figure also compares three schedules for the tuning parameter A_T : $0.5 \log \log T$, $\log \log T$, and $2 \log \log T$. Across all six models, the three RMSE curves are close and exhibit similar slopes, indicating that the convergence rate is robust to the choice of A_T within this range. The differences across schedules are mostly level shifts, so the precise constant in front of $\log \log T$ is not critical for achieving the minimax rate.

6 Empirical illustration

An outstanding feature of the method depicted in Dobrev & Schaumburg [27] is that the DS estimator can effectively capture the fastest speed of information transmission between two geographically separated markets, which is typically close to the speed of light. Specifically, they analyzed the lead-lag relationships between the cash and futures markets for the 10-Year U.S. Treasury Note and for the S&P 500 index. The DS estimator stably detected sharp peaks of the cross-market activity measures at 5 milliseconds, which is consistent with the optical propagation time between the futures exchange (in Aurora, Illinois) and the cash market platform (in Secaucus, New Jersey). In this section, we investigate whether this finding continues to

hold even for geographically closer markets, for which sub-millisecond estimates are required to detect such relationships.

More precisely, we examine the lead-lag relationships between the quotes of a single stock on two different exchanges: the NASDAQ (located in Carteret, New Jersey) and BATS (located in Secaucus, New Jersey). According to [67, Table 2], the optical propagation time between the NASDAQ and BATS exchanges is approximately 0.1 milliseconds. We obtain the timestamps of updates of the best quotes on each exchange in August 2015 from the Daily TAQ dataset, which provides every quote reported to the consolidated tape by all Consolidated Trade Association (CTA) and Unlisted Trading Privileges (UTP) participants. According to [8], the microsecond timestamps were fully implemented in this dataset on August 6, 2015. For this reason, we focus on the sample period beginning on August 6, 2015, comprising 18 trading days. Our analysis covers the component stocks of the NASDAQ-100 in 2015, totally 108 stocks. We restrict attention to transactions occurring between 9:45 and 15:45, discarding the first and last 15 minutes of the trading day in order to avoid non-stationarities commonly observed at the open and close.

In the Daily TAQ data, each quote record contains two timestamps: *Time* and *Participant Timestamp*, which refer to the timestamps published by Securities Information Processors (SIPs) and exchange matching engines, respectively. Following [8], we refer to the former as the *SIP timestamp* and the latter as the *participant timestamp*. See [8, Section 2] and [35, Section 4] for the institutional background. In this study, we use the participant timestamp because our preliminary analysis suggests that the SIP timestamp is heavily contaminated by *reporting latencies* in the terminology of [8]. Specifically, even when multiple market events occur simultaneously and share the same participant timestamp, they often receive different SIP timestamps, causing artificial misalignment across market events [56, 62, 68]. Moreover, reporting latencies fluctuate dynamically due to various latency sources, and their distribution is heavy-tailed (cf. [44, 56] and [8, Appendix]), making it difficult to disentangle their effects from genuine lead-lag behavior. For these reasons, we rely on participant timestamps. Developing a lead-lag estimator that is robust to such timestamp contamination would be an interesting direction for future research.

For each trading day and for each stock, we compute both our kernel estimator $\hat{\theta}_h$ and the DS estimator $\hat{\theta}_h^{DS}$. For the kernel estimator, we use the triangular kernel and select the bandwidth via the Lepski type method proposed in Section 4.1, with $\mathcal{H}_T = \{1 \mu\text{s}, 10 \mu\text{s}, 100 \mu\text{s}, 1000 \mu\text{s}\}$, $A_T = \log \log T$ and $T = 21600$ (the number of seconds in 6 trading hours). For the DS estimator, we consider two bucket sizes: $h = 1 \mu\text{s}$ and $h = 100 \mu\text{s}$. The former corresponds to the minimum time unit, as suggested in [27], whereas the latter is motivated by the physical transmission time of approximately $100 \mu\text{s}$ between the two exchanges (cf. [67, Table 2]). We set $r = 10 \text{ ms}$ for the search range for lead-lag parameters.

Fig. 4 presents violin plots of the lead-lag time estimates for the three estimators. The estimates of $\hat{\theta}_h$ cluster around several values, most notably around $95 \mu\text{s}$ and $130 \mu\text{s}$. These values have clear physical interpretations: According to [67, Table 2], the transmission time between NASDAQ and BATS is approximately $95 \mu\text{s}$ via hybrid laser link and $128 \mu\text{s}$ via fiber optic cable. This also suggests that, in our sample, NASDAQ generally leads BATS in updating best quotes, which is an intuitive result given that all the stocks analyzed are listed on NASDAQ, and NASDAQ tends to have greater market participation.

We observe a similar clustering pattern for the DS estimator with $h = 1 \mu\text{s}$, although these estimates appear to cluster slightly more around $130 \mu\text{s}$ than $95 \mu\text{s}$. However, they also exhibit a few negative “outliers”, an issue not present in the kernel estimator. Using a larger bucket size $h = 100 \mu\text{s}$ eliminates such outliers, but the coarse discretization inherent in the DS estimator significantly distorts the estimated lead-lag parameters.

To highlight the differences between our estimator and the DS estimator with $h = 1 \mu\text{s}$, Fig. 5 presents a scatter plot of the two sets of estimates, color-coded by $\sqrt{n_1 n_2}$, the geometric mean of the sample sizes. The two estimators yield similar values in many cases, but their estimates diverge as one or both of n_1 and n_2 become small. This observation aligns with our theoretical finding that the bucket size in the DS estimator should be increased when the sample size decreases (cf. the discussion following Theorem 3.1).

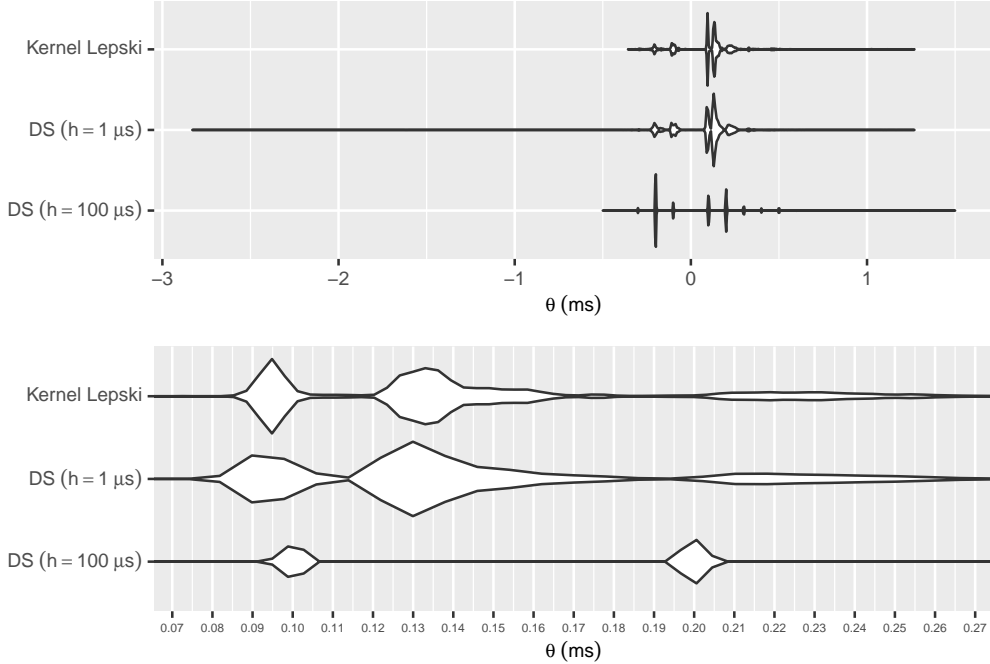


Figure 4: Violin plots of the daily lead-lag time estimates between quotes on the NASDAQ and BATS exchanges, computed for all the component stocks of the NASDAQ-100 in August 6–31, 2015. The top panel shows the entire plots, while the bottom panel zooms in on the interval from 0.07 ms to 0.27 ms. The smoothing bandwidths for the violin plots are selected by Sheather & Jones [64]’s method implemented as the R function `bw.SJ()`. The horizontal axis is expressed in milliseconds. A positive estimate implies that the NASDAQ leads the BATS and vice versa.

7 Concluding remarks

In this paper, we have established a theoretical foundation for timestamp-based lead-lag analysis from a point process perspective. Within this framework, the method of Dobrev & Schaumburg [27] for analyzing lead-lag relationships can be interpreted as an estimator of the cross-pair correlation function (CPCF) of the bivariate point process generated by two timestamp series. Accordingly, the prevailing lead-lag time is naturally defined as the location of the sharpest peak of this CPCF. We have proposed estimating this

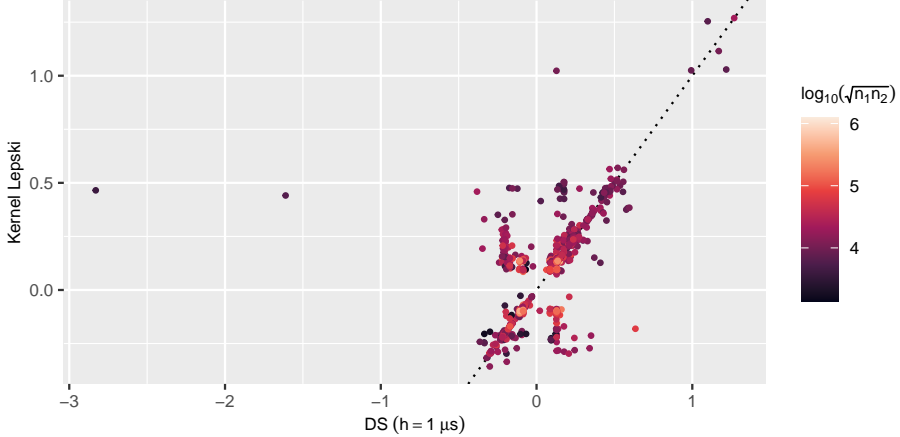


Figure 5: Scatter plot of the estimates of $\hat{\theta}_h^{DS}$ with $h = 1 \mu s$ versus $\hat{\theta}_{\hat{h}}$, color-coded by the geometric mean of the sample sizes. The values are expressed in milliseconds. The dotted line is the 45-degree line.

lead-lag time by maximizing a kernel density estimator of the CPCF. Theoretically, our estimator nearly attains the optimal convergence rate for estimating the lead-lag time, provided that the bandwidth of the kernel estimator is chosen appropriately. To this end, we have introduced a Lepski type bandwidth selection method. In practice, our procedure addresses several shortcomings of the Dobrev–Schaumburg estimator that arise from its discrete nature. We have demonstrated the superior performance of our estimator through comprehensive simulation studies and an illustrative empirical analysis.

Finally, we discuss several directions for future research to extend the applicability of our framework. First, extending the proposed method to non-stationary settings is of practical interest. Since financial market activity typically varies over time, the stationarity assumption imposed in this study may be restrictive for certain empirical applications. A promising avenue is to adopt the concept of transition-invariant cross-pair correlation function (see, e.g., [63]), which allows time-varying intensities while preserving a stable lead-lag structure that depends only on the time lag. Developing similar methods for such inhomogeneous settings would allow more accurate estimation of the lead-lag time. Second, in practical applications, timestamp series may be contaminated by observation noise. In such cases, a noise-robust estimator of the lead-lag parameter is required. This problem is closely related to deconvolution, which has been studied by [21] in the context of intensity function estimation for point processes and by [54] in the context of mode estimation for i.i.d. data. Third, empirical CPCF estimates for high-frequency timestamps often exhibit multiple peaks. These naturally arise because information transmission between two markets is bidirectional (as documented in [27]) and because transmission speeds differ across market participants. While this paper focuses solely on the sharpest peak, identifying all “significant” peaks would also be of interest. Similar questions have been studied in the classical literature on mode estimation; see [17, Section 3] and references therein. Fourth, it is also worth investigating how the lead-lag parameter is affected by order types, size, and market conditions such as spread and depth. By treating these attributes as marks, we can analyze the lead-lag relationships between marked point processes.

Appendix

A Proofs

Throughout the discussion, we use the following notation and convention. For two real numbers x, y , we write $x \lesssim y$ if $x \leq Cy$ for some constant $C > 0$ depending only on $r, \alpha, \alpha_0, \delta, b, (B_p)_{p \geq 1}, (B_{p,q})_{p,q \geq 1}, \varepsilon$ and $\|K\|_\infty$. For a real-valued function f defined on $[-r_1, r_1]$, we write $\|f\|_{L^p} = \|f\|_{L^p([-r_1, r_1])}$ for each $p \in [1, \infty]$ for short. We set $g_0 \equiv 1$ whenever [A2](i) is assumed.

A.1 Preliminaries

First, we can easily deduce from the definition of the cross-intensity function (3.1) that

$$\mathbb{E} \left[\int_{D \times \mathbb{R}} \varphi(y - x) N_1(dx) N_2(dy) \right] = \text{Leb}(D) \lambda_1 \lambda_2 \int_{\mathbb{R}} \varphi(u) g(u) du$$

for any Borel function $\varphi : \mathbb{R} \rightarrow [0, \infty]$ and $D \in \mathcal{B}(\mathbb{R})$. We refer to this identity as Campbell's formula in the following.

Next, we prove two auxiliary estimates that play a basic role throughout our discussion. The first is a moment inequality for a sum of dependent random variables in terms of the α -mixing coefficients (3.2) and is a simple consequence of [30, Theorem 2] with a truncation argument.

Lemma A.1. *Let $(X_j)_{j=0}^{T-1}$ be a sequence of random variables such that X_j is $\sigma(N \cap (I_j \oplus r_1))$ -measurable for all j . Suppose also that $\max_{0 \leq j \leq T-1} \mathbb{E}[X_j^q] < \infty$ for some even integer $q \geq 2$. Then, there exists a constant C_q depending only on q such that for any $M, \tau > 0$,*

$$\begin{aligned} \left\| \sum_{j=0}^{T-1} (X_j - \mathbb{E}[X_j]) \right\|_q &\leq C_q \left\{ \left(T\tau M \max_{0 \leq j \leq T-1} \mathbb{E}[|X_j|] + TM^2 \sum_{m=\tau}^{\infty} \alpha_{q,q}^N(m; r_1) \right)^{1/2} \right. \\ &\quad \left. + T^{1/q} M \left(\sum_{m=0}^{\infty} (m+1)^{q-2} \alpha_{q,q}^N(m; r_1) \right)^{1/q} \right\} + 2T \max_{0 \leq j \leq T-1} \left\| X_j 1_{\{|X_j| > M\}} \right\|_q. \end{aligned}$$

Proof. Set $Y_j := X_j 1_{\{|X_j| \leq M\}}$ for $j = 0, 1, \dots, T-1$. By the triangle inequality,

$$\begin{aligned} \left\| \sum_{j=0}^{T-1} (X_j - \mathbb{E}[X_j]) - \sum_{j=0}^{T-1} (Y_j - \mathbb{E}[Y_j]) \right\|_q &\leq \sum_{j=0}^{T-1} \left\| X_j 1_{\{|X_j| > M\}} - \mathbb{E}[X_j 1_{\{|X_j| > M\}}] \right\|_q \\ &\leq 2T \max_{0 \leq j \leq T-1} \left\| X_j 1_{\{|X_j| > M\}} \right\|_q. \end{aligned} \tag{A.1}$$

Meanwhile, for any integers $0 \leq j_1 \leq \dots \leq j_p \leq T-1$ such that $j_{k+1} - j_k = m$ for some $0 \leq k < p$ and $m \geq 0$, we have

$$|\text{Cov}[Y_{j_1} \dots Y_{j_k}, Y_{j_{k+1}} \dots Y_{j_p}]| \leq \min \left\{ 2M^{p-1} \max_{0 \leq j \leq T-1} \mathbb{E}[|X_j|], 4M^p \alpha_{p,p}^N(m; r_1) \right\},$$

where the second upper bound follows by the covariance inequality under strong mixing (see e.g. Lemma 3 in [29, Section 1.2]). Hence, we can apply [30, Theorem 2] to Y_j with $M = M, \gamma = C = 1$ and

$$\theta_m = \min \left\{ M \max_{0 \leq j \leq T-1} \mathbb{E}[|X_j|], 4M^2 \alpha_{q,q}^N(m; r_1) \right\}$$

in their notation. Hence, there exists a constant C_q depending only on q such that

$$\begin{aligned} \mathbb{E} \left[\left| \sum_{j=0}^{T-1} (Y_j - \mathbb{E}[Y_j]) \right|^q \right] &\leq C_q \left\{ \left(T \sum_{m=0}^{T-1} \theta_m \right)^{q/2} + M^{q-2} T \sum_{m=0}^{T-1} (m+1)^{q-2} \theta_m \right\} \\ &\leq C_q \left\{ \left(2T\tau M \max_{0 \leq j \leq T-1} \mathbb{E}[|X_j|] + 4TM^2 \sum_{m=\tau}^{\infty} \alpha_{q,q}^N(m; r_1) \right)^{q/2} \right. \\ &\quad \left. + 4TM^q \sum_{m=0}^{\infty} (m+1)^{q-2} \alpha_{q,q}^N(m; r_1) \right\}. \end{aligned}$$

Combining this with (A.1) gives the desired result. \square

The second is an estimate for the kernel-smoothed CPCF.

Lemma A.2. *Suppose that K is bounded and supported on $[-1, 1]$. For $h \in (0, 1]$, define a function $f_h : \mathbb{R} \rightarrow [0, \infty)$ as*

$$f_h(u) = \int_{\mathbb{R}} K_h(v-u)g(v)dv = \int_{\mathbb{R}} K(t)g(u+ht)dt, \quad u \in \mathbb{R}. \quad (\text{A.2})$$

Suppose also that there exist constants $\theta^* \in [-r, r]$, $\tilde{\alpha} \in (0, 1]$, $b > 1$ and a function $g_0 \in L^{\frac{1}{1-\tilde{\alpha}}}([-r_1, r_1])$ such that

$$g(u) \leq b \{ g_0(u) + |u - \theta^*|^{\tilde{\alpha}-1} \} \quad \text{for all } u \in [-r_1, r_1]. \quad (\text{A.3})$$

Then we have

$$f_h(u) \leq 2^{\tilde{\alpha}} \|K\|_{\infty} b \left(\|g_0\|_{L^{1/(1-\tilde{\alpha})}} + \frac{2}{\tilde{\alpha}} \right) h^{\tilde{\alpha}-1} \quad \text{for all } u \in [-r, r].$$

Proof. Fix $u \in [-r, r]$. (A.3) gives

$$f_h(u) \leq b \left(\int_{\mathbb{R}} K_h(v-u)g_0(v)dv + \int_{\mathbb{R}} K(t)|u - \theta^* + ht|^{\tilde{\alpha}-1} dt \right) =: b(I + II).$$

Since K_h is supported on $[-h, h] \subset [-1, 1]$, we can rewrite I as

$$I = \int_{-r_1}^{r_1} K_h(v-u)g_0(v)dv.$$

Hence, Young's convolution inequality gives $I \leq \|K_h\|_{L^{1/\tilde{\alpha}}} \|g_0\|_{L^{1/(1-\tilde{\alpha})}}$. Since

$$\|K_h\|_{L^{1/\tilde{\alpha}}} \leq \left(2h \|K_h\|_{\infty}^{1/\tilde{\alpha}} \right)^{\tilde{\alpha}} \leq 2^{\tilde{\alpha}} h^{\tilde{\alpha}-1} \|K\|_{\infty},$$

we obtain

$$I \leq 2^{\tilde{\alpha}} h^{\tilde{\alpha}-1} \|K\|_{\infty} \|g_0\|_{L^{1/(1-\tilde{\alpha})}}. \quad (\text{A.4})$$

Meanwhile, for any $c \in \mathbb{R}$, a straightforward computation shows

$$\int_{-1}^1 |c + ht|^{\tilde{\alpha}-1} dt = \begin{cases} \frac{|c+h|^{\tilde{\alpha}} - |c-h|^{\tilde{\alpha}}}{\tilde{\alpha}h} & \text{if } |c| > h, \\ \frac{|c+h|^{\tilde{\alpha}} + |c-h|^{\tilde{\alpha}}}{\tilde{\alpha}h} & \text{if } |c| \leq h. \end{cases}$$

Noting that $|x^{\tilde{\alpha}} - y^{\tilde{\alpha}}| \leq |x - y|^{\tilde{\alpha}}$ for any $x, y \geq 0$, we obtain

$$\sup_{c \in \mathbb{R}} \int_{-1}^1 |c + ht|^{\tilde{\alpha}-1} dt \leq \frac{2^{1+\tilde{\alpha}}}{\tilde{\alpha}} h^{\tilde{\alpha}-1}. \quad (\text{A.5})$$

Therefore, $II \leq \|K\|_\infty \frac{2^{1+\tilde{\alpha}}}{\tilde{\alpha}} h^{\tilde{\alpha}-1}$ since K is supported on $[-1, 1]$. Combining this with (A.4) gives the desired result. \square

A.2 Proof of Proposition 3.1

In the following two lemmas, we deal with the numerator and denominator of $\mathcal{X}_h^{\text{rel}}(\ell)$ separately.

Lemma A.3. *Assume [A1]. Suppose that there exist constants $\theta^* \in [-r, r]$, $\tilde{\alpha} \in (0, 1]$, $b > 1$ and a function $g_0 \in L^{1/(1-\tilde{\alpha})}([-r_1, r_1])$ such that (A.3) holds. Assume also $h = h_T \asymp T^{-\gamma}$ as $T \rightarrow \infty$ for some $\gamma > 0$. Then, for any $\varepsilon > 0$,*

$$\mathbb{E} \left[\max_{\ell \in \mathcal{G}_h} \left| \mathcal{X}_h^{\text{raw}}(\ell) - \frac{T}{h} \mathbb{E}[1_{\{N_1(I_0^h) > 0, N_2(I_\ell^h) > 0\}}] \right| \right] = O \left(1 + \sqrt{Th^{\tilde{\alpha}-\varepsilon}} \right). \quad (\text{A.6})$$

Proof. Set

$$\mathcal{X}_h^0(\ell) := \sum_{k=0}^{T/h-1} 1_{\{N_1(I_k^h) > 0, N_2(I_{k+\ell}^h) > 0\}}.$$

Since

$$\begin{aligned} |\mathcal{X}_h^{\text{raw}}(\ell) - \mathcal{X}_h^0(\ell)| &\leq \sum_{k=0}^{|\ell|-1} 1_{\{N_1(I_k^h) > 0\}} + \sum_{k=T/h-|\ell|}^{T/h-1} 1_{\{N_1(I_k^h) > 0\}} \\ &\leq N_1((0, |\ell| h]) + N_1((T - |\ell| h, T]), \end{aligned}$$

we have

$$\mathbb{E} \left[\max_{\ell \in \mathcal{G}_h} |\mathcal{X}_h^{\text{raw}}(\ell) - \mathcal{X}_h^0(\ell)| \right] \leq \mathbb{E}[N_1((0, r))] + \mathbb{E}[N_1((T - r, T))] = 2\lambda_1 r = O(1). \quad (\text{A.7})$$

Also, $\mathbb{E}[\mathcal{X}_h^0(\ell)] = (T/h) \mathbb{E}[1_{\{N_1(I_0^h) > 0, N_2(I_\ell^h) > 0\}}]$ by stationarity. Therefore, (A.6) follows once we show

$$\mathbb{E} \left[\max_{\ell \in \mathcal{G}_h} |\mathcal{X}_h^0(\ell) - \mathbb{E}[\mathcal{X}_h^0(\ell)]| \right] = O \left(\sqrt{Th^{\tilde{\alpha}-\varepsilon}} \right).$$

For any $p > 1$, Jensen's inequality gives

$$\begin{aligned} \mathbb{E} \left[\max_{\ell \in \mathcal{G}_h} |\mathcal{X}_h^0(\ell) - \mathbb{E}[\mathcal{X}_h^0(\ell)]| \right] &\leq \left\| \max_{\ell \in \mathcal{G}_h} |\mathcal{X}_h^0(\ell) - \mathbb{E}[\mathcal{X}_h^0(\ell)]| \right\|_p \\ &\leq |\mathcal{G}_h|^{1/p} \max_{\ell \in \mathcal{G}_h} \|\mathcal{X}_h^0(\ell) - \mathbb{E}[\mathcal{X}_h^0(\ell)]\|_p. \end{aligned}$$

Let p be an even integer such that $p \geq \frac{4}{\varepsilon(1-\gamma)}$. Then we have $|\mathcal{G}_h|^{1/p} = O(h^{-\varepsilon/4})$. Therefore, it suffices to prove

$$\max_{\ell \in \mathcal{G}_h} \|\mathcal{X}_h^0(\ell) - \mathbb{E}[\mathcal{X}_h^0(\ell)]\|_p = O \left(\sqrt{Th^{\tilde{\alpha}-\varepsilon/2}} \right). \quad (\text{A.8})$$

For each $\ell \in \mathcal{G}_h$, set

$$Y_j(\ell) := \sum_{k=j/h}^{(j+1)/h-1} 1_{\{N_1(I_k^h) > 0, N_2(I_{k+\ell}^h) > 0\}},$$

so that $\mathcal{X}_h^0(\ell) = \sum_{j=0}^{T-1} Y_j(\ell)$. Observe that $Y_j(\ell)$ is $\sigma(N \cap (I_j \oplus r))$ -measurable. Also, since

$$Y_j(\ell) \leq \sum_{k=j/h}^{(j+1)/h-1} N_1(I_k^h) = N_1(I_j),$$

[A1](i) yields

$$\sup_j \|Y_j(\ell)\|_q \leq \|N_1(I_j)\|_q \lesssim \lambda_1 \quad (\text{A.9})$$

for any $q \geq 1$. Therefore, applying Lemma A.1 to $(Y_j(\ell))_{j=0}^{T-1}$ with $M = h^{-\varepsilon/4}$ and $\tau = \lfloor h^{-\varepsilon/4} \rfloor$ gives

$$\begin{aligned} \|\mathcal{X}_h^0(\ell) - \mathbb{E}[\mathcal{X}_h^0(\ell)]\|_p &\leq C_p \left\{ \left(Th^{-\varepsilon/2} \mathbb{E}[Y_0(\ell)] + Th^{-\varepsilon/2} \sum_{m=\lfloor h^{-\varepsilon/4} \rfloor}^{\infty} \alpha_{p,p}^N(m; r_1) \right)^{1/2} \right. \\ &\quad \left. + T^{1/p} h^{-\varepsilon/4} \left(\sum_{m=0}^{\infty} (m+1)^{p-2} \alpha_{p,p}^N(m; r_1) \right)^{1/p} \right\} + 2T \left\| Y_0(\ell) 1_{\{Y_0(\ell) > h^{-\varepsilon/4}\}} \right\|_p, \end{aligned}$$

where C_p is a constant depending only on p and λ_1 . By [A1](ii),

$$\sum_{m=\lfloor h^{-\varepsilon/4} \rfloor}^{\infty} \alpha_{p,p}^N(m; r_1) = O(h^{\tilde{\alpha}}) \quad \text{and} \quad \sum_{m=0}^{\infty} (m+1)^{p-2} \alpha_{p,p}^N(m; r_1) = O(1).$$

Also, we have $\|Y_0(\ell) 1_{\{Y_0(\ell) > h^{-\varepsilon/4}\}}\|_p \leq h^{p\varepsilon/4} (\mathbb{E}[Y_0(\ell)^{p^2+p}])^{1/p} = O(T^{-1})$ by (A.9). Therefore, (A.8) follows once we show

$$\max_{\ell} \mathbb{E}[Y_0(\ell)] = O(h^{\tilde{\alpha}}). \quad (\text{A.10})$$

Observe that

$$\mathbb{E}[Y_0(\ell)] = h^{-1} \mathbb{E}[1_{\{N_1(I_0^h) > 0, N_2(I_{\ell}^h) > 0\}}] \leq h^{-1} \mathbb{E}[N_1(I_0^h) N_2(I_{\ell}^h)]$$

and

$$\begin{aligned} \mathbb{E}[N_1(I_0^h) N_2(I_{\ell}^h)] &= \lambda_1 \lambda_2 \int_{\mathbb{R}^2} 1_{I_0^h}(x) 1_{I_{\ell}^h}(x+u) g(u) dx du \\ &= \lambda_1 \lambda_2 h^2 \int_{\mathbb{R}} K_h^{\text{tri}}(u - \ell h) g(u) du. \end{aligned} \quad (\text{A.11})$$

Therefore, (A.10) follows from Lemma A.2. \square

Lemma A.4. *Assume [A1]. Then,*

$$\begin{aligned} \max_{\ell \in \mathcal{G}_h} \left| \frac{1}{T} \sum_{k=|\ell|}^{T/h-1-|\ell|} 1_{\{N_1(I_k^h) > 0\}} - \frac{\mathbb{P}(N_1(I_0^h) > 0)}{h} \right| &= O_p \left(\frac{1}{\sqrt{T}} \right), \\ \max_{\ell \in \mathcal{G}_h} \left| \frac{1}{T} \sum_{k=|\ell|}^{T/h-1-|\ell|} 1_{\{N_2(I_{k+\ell}^h) > 0\}} - \frac{\mathbb{P}(N_2(I_0^h) > 0)}{h} \right| &= O_p \left(\frac{1}{\sqrt{T}} \right) \end{aligned} \quad (\text{A.12})$$

and

$$\max_{\ell \in \mathcal{G}_h} \left| \frac{1}{T} \min \left\{ \sum_{k=|\ell|}^{T/h-1-|\ell|} 1_{\{N_1(I_k^h) > 0\}}, \sum_{k=|\ell|}^{T/h-1-|\ell|} 1_{\{N_2(I_{k+\ell}^h) > 0\}} \right\} - \lambda_1 \wedge \lambda_2 \right| \rightarrow^p 0 \quad (\text{A.13})$$

as $T \rightarrow \infty$.

Proof. (A.13) follows from (A.12) and the definition of intensity (cf. Eq.(3.3.4) of [23]), so it remains to prove (A.12). We only prove the first equation of (A.12) because the second can be shown by almost the same argument.

First, the same argument as in the proof of (A.7) gives

$$\mathbb{E} \left[\max_{\ell \in \mathcal{G}_h} \left| \sum_{k=|\ell|}^{T/h-1-|\ell|} 1_{\{N_1(I_k^h) > 0\}} - \sum_{k=0}^{T/h-1} 1_{\{N_1(I_k^h) > 0\}} \right| \right] = O(1).$$

Hence it suffices to show

$$\frac{1}{T} \sum_{k=0}^{T/h-1} 1_{\{N_1(I_k^h) > 0\}} = \frac{\mathbb{P}(N_1(I_0^h) > 0)}{h} + O_p \left(\frac{1}{\sqrt{T}} \right). \quad (\text{A.14})$$

We rewrite the left hand side as

$$\frac{1}{T} \sum_{k=0}^{T/h-1} 1_{\{N_1(I_k^h) > 0\}} = \frac{1}{T} \sum_{j=0}^{T-1} X_j,$$

where $X_j := \sum_{k=j/h}^{(j+1)/h-1} 1_{\{N_1(I_k^h) > 0\}}$. Observe that X_j is $\sigma(N \cap I_j)$ -measurable. Hence,

$$\text{Var} \left[\sum_{j=0}^{T-1} X_j \right] \leq \sum_{j,m=0}^{T-1} |\text{Cov}[X_j, X_{j+m}]| \leq 8 \sum_{j,m=0}^{T-1} \|X_j\|_4 \|X_m\|_4 \sqrt{\alpha_{1,1}(m; 0)} \lesssim T \|X_0\|_4^2,$$

where the second inequality follows by Theorem 3 in [29, Section 1.2] and the third by [A1](ii). Since $|X_0| \leq N_1(I_0)$, we obtain

$$\sum_{j=0}^{T-1} X_j = \sum_{j=0}^{T-1} \mathbb{E}[X_j] + O_p(\sqrt{T}) = \frac{T}{h} \mathbb{E}[1_{\{N_1(I_0^h) > 0\}}] + O_p(\sqrt{T}).$$

Since $\mathbb{E}[1_{\{N_1(I_0^h) > 0\}}] = \mathbb{P}(N_1(I_0^h) > 0)$, we obtain (A.14). \square

Proof of Proposition 3.1. Since g is bounded, (A.3) holds for $b = \sup_{x \in \mathbb{R}} |g(x)|$, $\tilde{\alpha} = 1$ and $g_0 \equiv 0$ (with θ^* arbitrary). Also, by assumption, $Th^{\tilde{\alpha}+\varepsilon} \rightarrow \infty$ as $T \rightarrow \infty$ for some $\varepsilon > 0$. Hence, Lemma A.3 gives

$$\max_{\ell \in \mathcal{G}_h} \left| \frac{\mathcal{X}_h^{\text{raw}}(\ell)}{Th} - \frac{\mathbb{E}[1_{\{N_1(I_0^h) > 0, N_2(I_\ell^h) > 0\}}]}{h^2} \right| \rightarrow^p 0. \quad (\text{A.15})$$

This particularly gives $\max_{\ell \in \mathcal{G}_h} \mathcal{X}_h^{\text{raw}}(\ell)/Th = O_p(1)$. Combining this with (A.13) gives

$$\max_{\ell \in \mathcal{G}_h} \left| \frac{\mathcal{X}_h^{\text{rel}}(\ell)}{h} - \frac{1}{\lambda_1 \wedge \lambda_2} \frac{\mathbb{E}[1_{\{N_1(I_0^h) > 0, N_2(I_\ell^h) > 0\}}]}{h^2} \right| \rightarrow^p 0.$$

Since $\lambda_1\lambda_2/(\lambda_1 \wedge \lambda_2) = \lambda_1 \vee \lambda_2$, we complete the proof once we show

$$\max_{\ell \in \mathcal{G}_h} \left| \frac{\mathbb{E}[1_{\{N_1(I_0^h) > 0, N_2(I_\ell^h) > 0\}}]}{h^2} - \lambda_1 \lambda_2 \int_{\mathbb{R}} K_h^{\text{tri}}(u - \ell h) g(u) du \right| = o(1).$$

Observe that

$$\begin{aligned} 0 &\leq \mathbb{E}[N_1(I_0^h)N_2(I_\ell^h)] - \mathbb{E}[1_{\{N_1(I_0^h) > 0, N_2(I_\ell^h) > 0\}}] \\ &= \mathbb{E}[(N_1(I_0^h) - 1)_+ \cdot N_2(I_\ell^h)] + \mathbb{E}[1_{\{N_1(I_0^h) > 0\}}(N_2(I_\ell^h) - 1)_+] \\ &\leq \mathbb{E}[N_1(I_0^h)(N_1(I_0^h) - 1)_+ \cdot N_2(I_\ell^h)] + \mathbb{E}[N_1(I_0^h)N_2(I_\ell^h)(N_2(I_\ell^h) - 1)_+] \\ &= \mathbb{E}[N_1(I_0^h)(N_1(I_0^h) - 1)N_2(I_\ell^h)] + \mathbb{E}[N_1(I_0^h)N_2(I_\ell^h)(N_2(I_\ell^h) - 1)]. \end{aligned}$$

Since we assume (3.4) for $\varpi = 1$, we obtain

$$\max_{\ell \in \mathcal{G}_h} \left| \mathbb{E}[N_1(I_0^h)N_2(I_\ell^h)] - \mathbb{E}[1_{\{N_1(I_0^h) > 0, N_2(I_\ell^h) > 0\}}] \right| = o(h^2).$$

Combining this with (A.11) gives the desired result. \square

A.3 Proof of Theorem 3.1

The following lemma summarizes identifiability conditions implied by [A2].

Lemma A.5. *Assume [K] and define the function f_h as in (A.2).*

(a) *Assume [A2](i). Then, for some $\sigma \in \{-1, 1\}$, there exist constants $A > 1$ and $0 < h_0 < 1$ depending only on α, b, δ such that*

$$f_h(\theta^* + \sigma v) - \sup_{u \in [-r, r]: |u - \theta^*| > Ah} f_h(u) \geq h^{\alpha-1} \quad \text{for all } h < h_0 \text{ and } v \in [h, 2h]. \quad (\text{A.16})$$

(b) *Assume [A2](ii). Then, for some $\sigma \in \{-1, 1\}$, there exist constants $A > 1, c > 0$ and $0 < h_0 < 1$ depending only on $\alpha, \alpha_0, b, \delta, K$ such that*

$$f_h(\theta^* + \sigma v) - \sup_{u \in [-r, r]: |u - \theta^*| > Ah} f_h(u) \geq ch^{\alpha-1} \quad \text{for all } h < h_0 \text{ and } v \in [0, h]. \quad (\text{A.17})$$

Proof. (a) By assumption, we have

$$\sup_{0 < \sigma(u - \theta^*) < \delta} \frac{g(\theta^*) - g(u)}{|u - \theta^*|^{\alpha-1}} \leq b \quad (\text{A.18})$$

for some $\sigma \in \{-1, 1\}$. Also, we have

$$g(u) \leq g(\theta^*) - b^{-1} \min \{1, |u - \theta^*|^{\alpha-1}\} \quad (\text{A.19})$$

for all $u \in \mathbb{R}$. Now, for any $A > 1$, we have by [K] and (A.19)

$$\sup_{u \in [-r, r]: |u - \theta^*| > Ah} f_h(u) \leq g(\theta^*) - b^{-1} \sup_{u \in [-r, r]: |u - \theta^*| > Ah} \int_{-1}^1 K(t) \min \{1, |u - \theta^* + ht|^{\alpha-1}\} dt$$

$$\leq g(\theta^*) - b^{-1} \min \{1, (A-1)^{\alpha-1} h^{\alpha-1}\}.$$

Meanwhile, by (A.18), we have for all $h < \delta/3$ and $v \in [h, 2h]$,

$$f_h(\theta^* + \sigma v) \geq g(\theta^*) - b \int_{-1}^1 K(t) |\sigma v + ht|^{\alpha-1} dt \geq g(\theta^*) - b(3h)^{\alpha-1}.$$

Combining these estimates gives

$$f_h(\theta^* + \sigma v) - \sup_{u \in [-r, r]: |u - \theta^*| > Ah} f_h(u) \geq b^{-1} \min \{1, (A-1)^{\alpha-1} h^{\alpha-1}\} - b(3h)^{\alpha-1}.$$

Therefore, if $A \geq 1 + (b + 3^{\alpha-1} b^2)^{1/(\alpha-1)}$ and $h < \min\{\delta/3, \{b(3^{\alpha-1} b + 1)\}^{-1/(\alpha-1)}\}$, we have (A.16).

(b) By assumption, we have

$$\inf_{0 < \sigma(u - \theta^*) < \delta} \frac{g(u)}{|u - \theta^*|^{\alpha-1}} \geq \frac{1}{b} \quad (\text{A.20})$$

for some $\sigma \in \{-1, 1\}$. Also, we have $\inf_{t \in [-\delta_0, \delta_0]} K(t) \geq K(0)/2 > 0$ for some $0 < \delta_0 < 1$ by [K]. Combining this with (A.20), we have for all $h < \delta/2$ and $v \in [0, h]$

$$f_h(\theta^* + \sigma v) \geq \frac{K(0)}{2b} \int_0^{\delta_0} |v + ht|^{\alpha-1} dt \geq \frac{K(0)}{2b} h^{\alpha-1} \int_0^{\delta_0} (1+t)^{\alpha-1} dt \geq \frac{K(0)\delta_0}{4b} h^{\alpha-1}.$$

Meanwhile, applying (A.4) to $\tilde{\alpha} = \alpha_0$ gives

$$\int_{\mathbb{R}} K_h(v - u) g_0(v) dv \leq 2^{\alpha_0} h^{\alpha_0-1} \|K\|_{\infty} b.$$

Hence, for any $A > 1$, we have by [A2] and [K]

$$\begin{aligned} \sup_{u \in [-r, r]: |u - \theta^*| > Ah} f_h(u) &\leq b \|K\|_{\infty} \left(2^{\alpha_0} h^{\alpha_0-1} b + \sup_{u \in [-r, r]: |u - \theta^*| > Ah} \int_{-1}^1 |u - \theta^* + ht|^{\alpha-1} dt \right) \\ &\leq 2b \|K\|_{\infty} \left(b h^{\alpha_0-1} + \frac{h^{\alpha-1}}{(A-1)^{1-\alpha}} \right). \end{aligned}$$

Therefore, if A is sufficiently large such that

$$\frac{2\|K\|_{\infty} b}{(A-1)^{1-\alpha}} \leq \frac{K(0)\delta_0}{8b},$$

we have

$$f_h(\theta^* + \sigma v) - \sup_{u \in [-r, r]: |u - \theta^*| > Ah} f_h(u) \geq \frac{K(0)\delta_0}{8b} h^{\alpha-1} - 2b^2 \|K\|_{\infty} h^{\alpha_0-1}.$$

Consequently, (A.17) holds if

$$h_0 \leq \min \left\{ \frac{\delta}{2}, \left(\frac{K(0)\delta_0}{32\|K\|_{\infty} b^3} \right)^{1/(\alpha_0-\alpha)} \right\} \quad \text{and} \quad c \leq \frac{K(0)\delta_0}{16b}.$$

This completes the proof. \square

Proof of Theorem 3.1. Observe that (A.3) holds for $\tilde{\alpha} = \alpha \wedge 1$ under [A2]. Hence, Lemma A.3 gives

$$h^{1-\alpha} \max_{\ell \in \mathcal{G}_h} \left| \frac{\mathcal{X}_h^{\text{raw}}(\ell)}{Th} - \frac{E[1_{\{N_1(I_0^h) > 0, N_2(I_\ell^h) > 0\}}]}{h^2} \right| = O\left(\frac{h^\alpha}{T} + \frac{1}{\sqrt{Th^{\beta_\alpha + \varepsilon}}}\right) \quad \text{for any } \varepsilon > 0,$$

where we used the identity $2\alpha - \alpha \wedge 1 = \beta_\alpha$. Also, by the proof of Proposition 3.1 and (3.4),

$$\max_{\ell \in \mathcal{G}_h} \left| \frac{E[N_1(I_0^h)N_2(I_\ell^h)] - E[1_{\{N_1(I_0^h) > 0, N_2(I_\ell^h) > 0\}}]}{h^2} \right| = o(h^{\alpha-1}).$$

Now, define the function f_h in (A.2) with $K = K^{\text{tri}}$. Recall that $h \asymp T^{-\gamma}$ with $0 < \gamma < 1/\beta_\alpha$. Therefore, combining the above two equations with (A.11), we obtain

$$h^{1-\alpha} \max_{\ell \in \mathcal{G}_h} \left| \frac{\mathcal{X}_h^{\text{raw}}(\ell)}{Th} - \lambda_1 \lambda_2 f_h(\ell h) \right| \rightarrow^p 0.$$

Combining this with Lemma A.2 particularly gives $\max_{\ell \in \mathcal{G}_h} \mathcal{X}_h^{\text{raw}}(\ell)/Th = O_p(h^{\tilde{\alpha}-1})$. Hence, by Lemma A.4,

$$h^{1-\alpha} \max_{\ell \in \mathcal{G}_h} \left| \frac{P(N_1(I_0^h) > 0) \wedge P(N_2(I_0^h) > 0)}{h^2} \mathcal{X}_h^{\text{rel}}(\ell) - \frac{\mathcal{X}_h^{\text{raw}}(\ell)}{Th} \right| \rightarrow^p 0.$$

Therefore, we have

$$h^{1-\alpha} \bar{\Delta}_T \rightarrow^p 0 \quad \text{as } T \rightarrow \infty, \quad (\text{A.21})$$

where

$$\bar{\Delta}_T := \max_{\ell \in \mathcal{G}_h} \left| \frac{P(N_1(I_0^h) > 0) \wedge P(N_2(I_0^h) > 0)}{\lambda_1 \lambda_2 h^2} \mathcal{X}_h^{\text{rel}}(\ell) - f_h(\ell h) \right|.$$

We turn to the main body of the proof. Consider the case $\alpha > 1$. Then, by Lemma A.5, for some $\sigma \in \{-1, 1\}$, there exist constants $A > 1$ and $0 < h_0 < 1$ depending only on α, b, δ such that (A.16) holds. We can find an integer ℓ^* such that $\ell^* h = \theta^* + \sigma v$ for some $v \in [h, 2h]$. Observe that $\ell^* \in \mathcal{G}_h$ for sufficiently small h . Then, since $\hat{\theta}_h^{\text{DS}}$ is a maximizer of $\mathcal{G}_h \ni \ell \mapsto \mathcal{X}_h^{\text{rel}}(\ell) \in [0, \infty)$, we have

$$\begin{aligned} P(|\hat{\theta}_h^{\text{DS}} - \theta^*| > (A+4)h) &\leq P(|\hat{\theta}_h^{\text{DS}} - \ell^* h| > (A+2)h) \\ &\leq P\left(\mathcal{X}_h^{\text{rel}}(\ell^*) \leq \max_{\ell \in \mathcal{G}_h: |\ell - \ell^*| > A+2} \mathcal{X}_h^{\text{rel}}(\ell)\right) \\ &\leq P\left(f_h(\ell^* h) \leq \max_{\ell \in \mathcal{G}_h: |\ell - \ell^*| > A+2} f_h(\ell h) + 2\bar{\Delta}_T\right) \\ &\leq P\left(f_h(\ell^* h) \leq \max_{\ell \in \mathcal{G}_h: |\ell h - \theta^*| > Ah} f_h(\ell h) + 2\bar{\Delta}_T\right). \end{aligned}$$

Hence, (A.16) gives $P(|\hat{\theta}_h^{\text{DS}} - \theta^*| > (A+4)h) \leq P(2\bar{\Delta}_T \geq h^{\alpha-1})$. Thus we obtain the desired result by (A.21).

Next, consider the case $\alpha < 1$. Then, by Lemma A.5, for some $\sigma \in \{-1, 1\}$, there exist constants $A > 1, c > 0$ and $0 < h_0 < 1$ depending only on $\alpha, \alpha_0, b, \delta$ such that (A.17) holds. We can find an integer ℓ^* such that $\ell^* h = \theta^* + \sigma v$ for some $v \in [0, h]$. Then, a similar argument to the above shows $P(|\hat{\theta}_h^{\text{DS}} - \theta^*| > (A+2)h) \rightarrow 0$ as $T \rightarrow \infty$. \square

A.4 Proof of Theorem 4.1

Set $\tilde{\alpha} := \alpha \wedge 1$. Note that $\tilde{\alpha} \leq \beta_\alpha$. Since the left hand side of (4.1) is always bounded by 1, we may assume $Th^{\beta_\alpha + \varepsilon} \geq 1$ without loss of generality.

Let us consider the following statistic:

$$\tilde{g}_h(u) := \frac{n_1}{T\lambda_1} \frac{n_2}{T\lambda_2} \hat{g}_h(u) = \frac{1}{T\lambda_1\lambda_2} \int_{(0,T]^2} K_h(y - x - u) N_1(dx) N_2(dy), \quad u \in \mathbb{R}.$$

Observe that $\hat{\theta}_h$ is also a maximizer of $\tilde{g}_h(u)$ over $u \in [-r, r]$. Also, we can rewrite it as $\tilde{g}_h(u) = \sum_{j=0}^{T-1} X_j^0(u)$, where

$$X_j^0(u) = \frac{1}{T\lambda_1\lambda_2} \int_{I_j \times (0,T]} K_h(y - x - u) N_1(dx) N_2(dy).$$

We introduce an edge-corrected version of $X_j^0(u)$ as

$$X_j(u) = \frac{1}{T\lambda_1\lambda_2} \int_{I_j \times \mathbb{R}} K_h(y - x - u) N_1(dx) N_2(dy).$$

It is not difficult to see that $(X_j(u))_{j \in \mathbb{Z}}$ is stationary. We first show that replacing $X_j^0(u)$ by $X_j(u)$ does not matter for our argument.

Lemma A.6. *Assume [A1]. Assume also that K is bounded and supported on $[-1, 1]$. Then,*

$$\mathbb{E} \left[\sup_{u \in [-r, r]} \left| \tilde{g}_h(u) - \sum_{j=0}^{T-1} X_j(u) \right| \right] \lesssim \frac{1}{Th}.$$

Proof. Since K_h is supported on $[-h, h] \subset [-1, 1]$, $X_j^0(u) = X_j(u)$ if $r_1 < j < T - 1 - r_1$ for any $u \in [-r, r]$. Therefore,

$$\left| \tilde{g}_h(u) - \sum_{j=0}^{T-1} X_j(u) \right| \leq \frac{\|K\|_\infty}{Th\lambda_1\lambda_2} \sum_{0 \leq j \leq r_1 \text{ or } T-1-r_1 \leq j \leq T-1} N_1(I_j) N_2(I_j \oplus r_1).$$

Hence, the desired result follows by [A1](i). \square

Next, set

$$\Delta_T(u) := \sum_{j=0}^{T-1} \{X_j(u) - \mathbb{E}[X_j(u)]\}, \quad u \in [-r, r].$$

Our next aim is to establish a sufficiently fast convergence of $\sup_{u \in [-r, r]} |\Delta_T(u)|$. We first develop pointwise moment bounds.

Lemma A.7. *Assume [A1] and [A2]. Assume also that K is bounded and supported on $[-1, 1]$. If an even integer $p > 2$ satisfies $Th^{p\varepsilon/4} \leq 1$, then*

$$h^{1-\tilde{\alpha}} \sup_{u \in [-r, r]} \|\Delta_T(u)\|_p \lesssim \frac{C_p}{\sqrt{Th^{\tilde{\alpha}+\varepsilon/2}}},$$

where C_p is a constant depending only on p .

Proof. Fix $u \in [-r, r]$. Since K_h is supported on $[-h, h] \subset [-1, 1]$, we can rewrite $X_j(u)$ as

$$X_j(u) = \frac{1}{T\lambda_1\lambda_2} \int_{I_j \times (I_j \oplus r_1)} K_h(y - x - u) N_1(dx) N_2(dy). \quad (\text{A.22})$$

Hence, $X_j(u)$ is $\sigma(N \cap (I_j \oplus r_1))$ -measurable for every j . Also, since $\|K_h\|_\infty \leq h^{-1} \|K\|_\infty$, we obtain for any $q > 1$

$$\max_{0 \leq j \leq T-1} \|X_j(u)\|_q = \|X_0(u)\|_q \lesssim \frac{1}{Th\lambda_1\lambda_2} \|N_1(I_0)N_2(I_0 \oplus r_1)\|_q \lesssim \frac{1}{Th}. \quad (\text{A.23})$$

Therefore, applying Lemma A.1 to $(X_j(u))_{j=0}^{T-1}$ with $M = h^{-\varepsilon/4}/(Th)$ and $\tau = \lfloor h^{-\varepsilon/4} \rfloor$ gives

$$\begin{aligned} \|\Delta_T(u)\|_p &\leq C_p \left\{ \left(\frac{h^{-\varepsilon/2}}{h} \mathbb{E}[|X_0(u)|] + \frac{h^{-\varepsilon/2}}{Th^2} \sum_{m=\lfloor h^{-\varepsilon/4} \rfloor}^{\infty} \alpha_{p,p}^N(m; r_1) \right)^{1/2} \right. \\ &\quad \left. + \frac{T^{1/p} h^{-\varepsilon/4}}{Th} \left(\sum_{m=0}^{\infty} (m+1)^{p-2} \alpha_{p,p}^N(m; r_1) \right)^{1/p} \right\} + 2T \left\| X_0(u) 1_{\{X_0(u) > h^{-\varepsilon/4}/(Th)\}} \right\|_p, \end{aligned}$$

where C_p is a constant depending only on p . By [A1](ii),

$$\sum_{m=\lfloor h^{-\varepsilon/4} \rfloor}^{\infty} \alpha_{p,p}^N(m; r_1) \lesssim h^{\tilde{\alpha}} \quad \text{and} \quad \sum_{m=0}^{\infty} (m+1)^{p-2} \alpha_{p,p}^N(m; r_1) \lesssim 1.$$

Also, since (A.3) holds under [A2], Campbell's formula and Lemma A.2 give

$$\mathbb{E}[X_0(u)] = \frac{1}{T} \int_{-1}^1 K(t) g(u + ht) dt \lesssim \frac{1}{T} \int_{-1}^1 (1 + |u - \theta^* + ht|^{\tilde{\alpha}-1}) dt \lesssim \frac{1}{Th^{1-\tilde{\alpha}}}. \quad (\text{A.24})$$

Moreover, by (A.23),

$$\left\| X_0(u) 1_{\{X_0(u) > h^{-\varepsilon/4}/(Th)\}} \right\|_p \leq \left(\frac{Th}{h^{-\varepsilon/4}} \right)^p (\mathbb{E}[X_0(u)^{p^2+p}])^{1/p} \lesssim \frac{h^{p\varepsilon/4}}{Th}.$$

Since $Th^{p\varepsilon/4} \leq 1$, we obtain

$$h^{1-\tilde{\alpha}} \|\Delta_T(u)\|_p \lesssim C_p \left(\frac{1}{\sqrt{Th^{\tilde{\alpha}+\varepsilon/2}}} + \frac{1}{Th^{\tilde{\alpha}+\varepsilon/2}} \right).$$

Since we assume $Th^{\tilde{\alpha}+\varepsilon/2} \geq Th^{\beta_\alpha+\varepsilon} \geq 1$, this gives the desired result. \square

To upgrade Lemma A.7 to a moment bound for $\sup_{u \in [-r,r]} |\Delta_T(u)|$, we need the following technical lemma.

Lemma A.8. *Let F be a bounded non-decreasing function on \mathbb{R} . For any $h, \rho > 0$, there exist finite points $-r = u_0 \leq u_1 \leq \dots \leq u_N = r$ and universal constants $C, d \geq 1$ such that $N \leq C\rho^{-d}$ and*

$$\sup_{u \in [-r,r]} \min_{0 \leq a \leq N-1} \int_{-r_1}^{r_1} \{F_h(v - u_a) - F_h(v - u_{a+1})\} g(v) dv \leq 2\rho \frac{\|F\|_\infty}{h} \int_{-r_1}^{r_1} g(u) du. \quad (\text{A.25})$$

Proof. Without loss of generality, we may assume $\int_{-r_1}^{r_1} g(u)du > 0$ since otherwise the asserted claim is trivial.

By the proof of [33, Proposition 3.6.12], $\mathcal{G} := \{F_h(\cdot - u) : u \in [-r, r]\}$ is a VC subgraph class of functions. Also, \mathcal{G} admits an envelope $\|F\|_\infty/h$. Therefore, by [33, Theorem 3.3.9], there exist finite points $-r = s_0 < s_1 < \dots < s_L = r$ and universal constants $C, d \geq 1$ such that $L \leq C\rho^{-d}$ and

$$\sup_{u \in [-r, r]} \min_{0 \leq a \leq L} \int_{\mathbb{R}} |F_h(v - u) - F_h(v - s_a)| Q(dv) \leq \rho \frac{\|F\|_\infty}{h}, \quad (\text{A.26})$$

where Q is a probability measure on $(\mathbb{R}, \mathcal{B}(\mathbb{R}))$ defined as

$$Q(A) = \frac{\int_{A \cap [-r_1, r_1]} g(u)du}{\int_{-r_1}^{r_1} g(u)du}, \quad A \in \mathcal{B}(\mathbb{R}).$$

Next, define a function $\psi : \mathbb{R} \rightarrow \mathbb{R}$ as

$$\psi(u) = \int_{-r_1}^{r_1} F_h(v - u)g(v)dv = \int_{\mathbb{R}} F(t)g(u + ht)1_{[-r_1, r_1]}(u + ht)dt, \quad u \in \mathbb{R}.$$

Then, (A.26) gives

$$\sup_{u \in [-r, r]} \min_{0 \leq a \leq L} |\psi(u) - \psi(s_a)| \leq \rho \frac{\|F\|_\infty}{h} \int_{-r_1}^{r_1} g(u)du.$$

Also, since g is non-negative and F is non-decreasing, ψ is non-increasing. Moreover, since $g1_{[-r_1, r_1]} \in L^1(\mathbb{R})$ and F is bounded, ψ is continuous (see e.g. [53, Lemma 1.8.1]). Consequently, for every $a = 0, \dots, L-1$, there exists a point $t_a \in [s_a, s_{a+1}]$ such that $\psi(t_a) = \{\psi(s_a) + \psi(s_{a+1})\}/2$ by the intermediate value theorem. Observe that $\psi(s_a) - \psi(t_a) = \psi(t_a) - \psi(s_{a+1}) = \{\psi(s_a) - \psi(s_{a+1})\}/2$. Moreover, since ψ is non-increasing,

$$\min_{0 \leq a' \leq L} |\psi(t_a) - \psi(s_{a'})| = \{\psi(s_a) - \psi(t_a)\} \wedge \{\psi(t_a) - \psi(s_{a+1})\} = \frac{\psi(s_a) - \psi(s_{a+1})}{2}.$$

Therefore, we obtain the desired points by setting $u_{2a} = s_a$ and $u_{2a+1} = t_a$ for $a = 0, \dots, L-1$ and $u_{2L} = s_L$. \square

Combining the previous two lemmas, we can derive the following uniform moment bound for $\Delta_T(u)$:

Lemma A.9. *Assume [A1] and [A2]. Assume also that K is of bounded variation and supported on $[-1, 1]$. If $h \leq \min\{T^{-\eta}, 1/2\}$ for some $\eta > 0$, then*

$$\mathbb{E} \left[h^{1-\tilde{\alpha}} \sup_{u \in [-r, r]} |\Delta_T(u)| \right] \lesssim \frac{C_\eta}{\sqrt{Th^{\tilde{\alpha}+\varepsilon}}},$$

where C_η depends only on η .

Proof. Since K is of bounded variation and supported on $[-1, 1]$, there exist two non-decreasing functions F_1, F_2 on \mathbb{R} such that $K = (F_1 - F_2)1_{[-1, 1]}$ and $|F_1| \vee |F_2| \leq \|K\|_\infty$. Therefore, without loss of generality, we may assume that K is of the form $K = F1_{[-1, 1]}$ with F a non-decreasing function on \mathbb{R} . In the remainder of the proof, we proceed in two steps.

Step 1. For $\rho = h/T^{1/\tilde{\alpha}}$, let $-r = u_0 \leq u_1 \leq \dots \leq u_N = r$ and $d \geq 1$ be as in Lemma A.8. Inserting the equi-spaced points $-r + k\rho$ ($k = 1, \dots, \lfloor 2r/\rho \rfloor$) into the sequence $(u_a)_{a=0}^N$ if necessary, we may assume $\max_{0 \leq a \leq N-1} (u_{a+1} - u_a) \leq \rho$ while (A.25) still holds. Note that this operation increases the number of points at most $\lfloor 2r/\rho \rfloor$, so we have $N \lesssim \rho^{-d}$.

For each $u \in [-r, r]$, set

$$\tilde{X}_j(u) := \frac{1}{T\lambda_1\lambda_2} \int_{I_j \times \mathbb{R}} 1_{[-h, h] \oplus \rho}(y - x - u) F_h(y - x - u) N_1(dx) N_2(dy), \quad j = 0, 1, \dots, T-1$$

and

$$\tilde{\Delta}_T(u) := \sum_{j=0}^{T-1} \left\{ \tilde{X}_j(u) - \mathbb{E}[\tilde{X}_j(u)] \right\}.$$

In Step 2, we will show

$$\mathbb{E} \left[h^{1-\tilde{\alpha}} \sup_{u \in [-r, r]} |\Delta_T(u)| \right] \lesssim \mathbb{E} \left[h^{1-\tilde{\alpha}} \max_{0 \leq a \leq N} |\tilde{\Delta}_T(u_a)| \right] + \frac{1}{\sqrt{Th^{\tilde{\alpha}}}}. \quad (\text{A.27})$$

Given this estimate, we can prove the claim of the lemma as follows. Since $N \lesssim \rho^{-d} \leq h^{-d\{1+1/(\tilde{\alpha}\eta)\}}$, we have $N^{1/p} \lesssim h^{-\varepsilon/4}$ for a sufficiently large even integer p depending only on α and η . Observe that Jensen's inequality gives

$$\mathbb{E} \left[h^{1-\tilde{\alpha}} \max_{0 \leq a \leq N} |\tilde{\Delta}_T(u_a)| \right] \leq h^{1-\tilde{\alpha}} \left(\mathbb{E} \left[\max_{0 \leq a \leq N} |\tilde{\Delta}_T(u_a)|^p \right] \right)^{1/p} \leq (N+1)^{1/p} h^{1-\tilde{\alpha}} \max_{0 \leq a \leq N} \|\tilde{\Delta}_T(u_a)\|_p.$$

Meanwhile, define a function $\tilde{K} : \mathbb{R} \rightarrow \mathbb{R}$ as $\tilde{K}(u) = 2F(2u)1_{[-1, 1] \oplus T^{-1/\tilde{\alpha}}}(2u)$ for $u \in \mathbb{R}$. Observe that \tilde{K} is supported on $[-1, 1]$ and bounded by $2\|K\|_\infty$. Moreover, we can rewrite $\tilde{X}_j(u)$ as

$$\tilde{X}_j(u) = \frac{1}{T\lambda_1\lambda_2} \int_{I_j \times \mathbb{R}} \tilde{K}_{2h}(y - x - u) N_1(dx) N_2(dy).$$

Therefore, we can apply Lemma A.7 to $\tilde{\Delta}_T(u)$ and thus obtain

$$\mathbb{E} \left[h^{1-\tilde{\alpha}} \max_{0 \leq a \leq N} |\tilde{\Delta}_T(u_a)| \right] \lesssim \frac{(N+1)^{1/p}}{\sqrt{Th^{\tilde{\alpha}+\varepsilon/2}}} \lesssim \frac{1}{\sqrt{Th^{\tilde{\alpha}+\varepsilon}}}.$$

Combining this with (A.27) gives the claim of the lemma.

Step 2. It remains to prove (A.27). Fix $u \in [-r, r]$. We can find an index $0 \leq a < N$ such that $u_a \leq u \leq u_{a+1}$. Since $u - u_a \leq u_{a+1} - u_a \leq \rho$ and F is non-decreasing, we have

$$X_j(u) = \frac{1}{T\lambda_1\lambda_2} \int_{I_j \times \mathbb{R}} 1_{[-h, h]}(y - x - u) F_h(y - x - u) N_1(dx) N_2(dy) \leq \tilde{X}_j(u_a)$$

for all j . Campbell's formula gives

$$\mathbb{E}[\tilde{X}_j(u_a)] = \frac{1}{T} \int_{\mathbb{R}} 1_{[-h, h] \oplus \rho}(v - u_a) K_h(v - u_a) g(v) dv$$

$$= \frac{1}{T} \int_{-r_1}^{r_1} 1_{[-h,h] \oplus \rho}(v - u_a) K_h(v - u_a) g(v) dv,$$

where the second equality follows from $u_a \in [-r, r]$ and $h + \rho \leq 2h \leq 1$. Observe that $1_{[-h,h] \oplus \rho}(v - u_a) = 1_{J_{h,u}}(v - u)$ with $J_{h,u} := ([-h, h] \oplus \rho) + (u_a - u)$. Note that $J_{h,u} \supset [-h, h]$ because $u - u_a \leq \rho$. Hence,

$$\left| \mathbb{E}[\tilde{X}_j(u_a)] - \frac{1}{T} \int_{-r_1}^{r_1} 1_{[-h,h]}(v - u) K_h(v - u_a) g(v) dv \right| \leq \frac{\|K\|_\infty}{Th} \int_{-r_1}^{r_1} 1_{J_{h,u} \setminus [-h,h]}(v - u) g(v) dv.$$

Noting that $\|g_0\|_{L^{1/(1-\tilde{\alpha}/2)}}$ $\lesssim 1$ by Jensen's inequality (if $\alpha < 1$) and $\int_{-r_1}^{r_1} |u - \theta^*|^{\frac{\alpha-1}{1-\tilde{\alpha}/2}} du \lesssim 1$ because $\frac{\alpha-1}{1-\tilde{\alpha}/2} > -1$, we have $\|g\|_{L^{1/(1-\tilde{\alpha}/2)}}$ $\lesssim 1$ by [A2]. Then, since $\text{Leb}(J_{h,u} \setminus [-h, h]) \lesssim \rho$, Young's inequality gives

$$\left| \mathbb{E}[\tilde{X}_j(u_a)] - \frac{1}{T} \int_{-r_1}^{r_1} 1_{[-h,h]}(v - u) K_h(v - u_a) g(v) dv \right| \lesssim \frac{\rho^{\tilde{\alpha}/2}}{Th}.$$

Meanwhile, by Campbell's formula again,

$$\mathbb{E}[X_j(u)] = \frac{1}{T} \int_{\mathbb{R}} 1_{[-h,h]}(v - u) K_h(v - u) g(v) dv.$$

Therefore, (A.25) gives

$$\left| \mathbb{E}[X_j(u)] - \frac{1}{T} \int_{-r_1}^{r_1} 1_{[-h,h]}(v - u) K_h(v - u_a) g(v) dv \right| \lesssim \frac{\rho}{Th}.$$

Consequently,

$$X_j(u) - \mathbb{E}[X_j(u)] \leq \tilde{X}_j(u_a) - \mathbb{E}[\tilde{X}_j(u_a)] + C_0 \frac{\rho^{\tilde{\alpha}/2}}{Th},$$

where $C_0 > 0$ is a constant depending only on $r, \alpha, \alpha_0, \delta, b, (B_p)_{p \geq 1}, (B_{p,q})_{p,q \geq 1}, \varepsilon$ and $\|K\|_\infty$. Similarly, we also have

$$X_j(u) - \mathbb{E}[X_j(u)] \geq \tilde{X}_j(u_{a+1}) - \mathbb{E}[\tilde{X}_j(u_{a+1})] - C_0 \frac{\rho^{\tilde{\alpha}/2}}{Th}.$$

Thus, we conclude

$$\sup_{u \in [-r, r]} |\Delta_T(u)| \leq \max_{0 \leq a \leq N} |\tilde{\Delta}_T(u_a)| + C_0 \frac{\rho^{\tilde{\alpha}/2}}{h}.$$

Therefore, (A.27) follows from the definition of ρ . \square

Proof of Theorem 4.1. Define the function f_h by (A.2) and set $\bar{\Delta}_T := \sup_{u \in [-r, r]} |\tilde{g}_h(u) - f_h(u)|$. Since $\mathbb{E}[X_j(u)] = f_h(u)$ for all j , Lemma A.6 gives

$$\mathbb{E}[\bar{\Delta}_T] \lesssim \mathbb{E} \left[\sup_{u \in [-r, r]} |\Delta_T(u)| \right] + \frac{1}{Th}. \quad (\text{A.28})$$

Now, consider the case $\alpha > 1$. Then, by Lemma A.5, for some $\sigma \in \{-1, 1\}$, there exist constants $A > 1$ and $0 < h_0 < 1$ depending only on α, b, δ such that (A.16) holds. Since $\hat{\theta}_h$ is a maximizer of $[-r, r] \ni u \mapsto \tilde{g}_h(u) \in [0, \infty)$, we have

$$\mathbb{P}(|\hat{\theta}_h - \theta^*| > Ah) \leq \mathbb{P} \left(\tilde{g}_h(\theta^* + \sigma h) \leq \sup_{u \in [-r, r]: |u - \theta^*| > Ah} \tilde{g}_h(u) \right)$$

$$\leq P \left(f_h(\theta^* + \sigma h) \leq \sup_{u \in [-r, r]: |u - \theta^*| > Ah} f_h(u) + 2\bar{\Delta}_T \right).$$

Therefore, (A.16) gives $P(|\hat{\theta}_h - \theta^*| > Ah) \leq P(2\bar{\Delta}_T \geq h^{\alpha-1})$. Hence, the desired result follows by Markov's inequality, (A.28) and Lemma A.9.

Next, consider the case $\alpha < 1$. Then, by Lemma A.5, for some $\sigma \in \{-1, 1\}$, there exist constants $A > 1, c > 0$ and $0 < h_0 < 1$ depending only on $\alpha, \alpha_0, b, \delta, K$ such that (A.17) holds. Since $\hat{\theta}_h$ is a maximizer of $[-r, r] \ni u \mapsto \tilde{g}_h(u) \in [0, \infty)$,

$$\begin{aligned} P(|\hat{\theta}_h - \theta^*| > Ah) &\leq P \left(\tilde{g}_h(\theta^*) \leq \sup_{u \in [-r, r]: |u - \theta^*| > Ah} \tilde{g}_h(u) \right) \\ &\leq P \left(f_h(\theta^*) \leq \sup_{u \in [-r, r]: |u - \theta^*| > Ah} f_h(u) + 2\bar{\Delta}_T \right) \\ &\leq P(2\bar{\Delta}_T \geq ch^{\alpha-1}), \end{aligned}$$

where the last line follows from (A.17). Therefore, the desired result follows by Markov's inequality, (A.28) and Lemma A.9 again. \square

A.5 Proof of Theorem 4.2

Below we assume T is sufficiently large T such that $j_{\min} \leq \log_a(T_{\max}^\gamma)$. For $0 < \gamma \leq \gamma_{\max}$, we write $h^*(\gamma)$ for the largest element $h \in \mathcal{H}_T$ such that $h \leq T^{-\gamma}$. Note that $h^*(\gamma)$ is well-defined because $\gamma \leq \gamma_{\max}$. Also, $ah^*(\gamma) > T^{-\gamma}$ for sufficiently large T by construction, so $h^*(\gamma) \asymp T^{-\gamma}$ as $T \rightarrow \infty$.

Lemma A.10. *Under the assumptions of Theorem 4.2, for any $0 < \gamma < 1/\beta_\alpha$, $P(\hat{h} > T^{-\gamma}) \rightarrow 0$ as $T \rightarrow \infty$.*

Proof. Write $h^* = h^*(\gamma)$ for short. Observe that

$$\begin{aligned} P(\hat{h} > T^{-\gamma}) &\leq P(\hat{h} > h^*) \leq P(\bar{d}(\mathcal{M}_{h^*}, \mathcal{M}_{h'}) > A_T h' \text{ for some } h' \in \mathcal{H}_T \text{ with } h' \geq h^*) \\ &\leq \sum_{h' \in \mathcal{H}_T: h' \geq h^*} P(\bar{d}(\mathcal{M}_{h^*}, \mathcal{M}_{h'}) > A_T h'). \end{aligned}$$

Since $\bar{d}(\mathcal{M}_{h^*}, \mathcal{M}_{h'}) \leq \bar{d}(\mathcal{M}_{h^*}, \{\theta^*\}) + \bar{d}(\mathcal{M}_{h'}, \{\theta^*\})$, we have

$$\begin{aligned} P(\hat{h} > T^{-\gamma}) &\leq \sum_{h' \in \mathcal{H}_T: h' \geq h^*} \{P(\bar{d}(\mathcal{M}_{h^*}, \{\theta^*\}) > A_T h'/2) + P(\bar{d}(\mathcal{M}_{h'}, \{\theta^*\}) > A_T h'/2)\} \\ &\leq 2|\mathcal{H}_T| \max_{h \in \mathcal{H}_T: h \geq h^*} P(\bar{d}(\mathcal{M}_h, \{\theta^*\}) > A_T h/2). \end{aligned}$$

For every $h \in \mathcal{H}_T$, we can find a random variable $\tilde{\theta}_h \in \mathcal{M}_h$ such that $|\tilde{\theta}_h - \theta^*| > A_T h/2$ on the event $\bar{d}(\mathcal{M}_h, \{\theta^*\}) > A_T h/2$. Hence,

$$P(\hat{h} > T^{-\gamma}) \leq 2|\mathcal{H}_T| \max_{h \in \mathcal{H}_T: h \geq h^*} P(|\tilde{\theta}_h - \theta^*| > A_T h/2).$$

Thus, for any $\varepsilon > 0$, Theorem 4.1 gives

$$P(\hat{h}_T > T^{-\gamma}) = O\left(|\mathcal{H}_T| \max_{h \in \mathcal{H}_T: h \geq h^*} \frac{1}{\sqrt{Th^{\beta_\alpha + \varepsilon}}}\right) = O\left(\frac{|\mathcal{H}_T|}{\sqrt{T(h^*)^{\beta_\alpha + \varepsilon}}}\right).$$

Since $\gamma < 1/\beta_\alpha$ and $|\mathcal{H}_T| = O(\log T)$, we obtain the desired result by taking ε so that $\gamma(\beta_\alpha + \varepsilon) < 1$. \square

Proof of Theorem 4.2. Let γ' be a constant such that $\gamma < \gamma' < 1/\beta_\alpha$. Then, $A_T T^{-\gamma'} = o(T^{-\gamma})$ by assumption. Hence it is enough to prove $P(|\hat{\theta}_{\hat{h}} - \theta^*| > 2A_T T^{-\gamma'}) \rightarrow 0$. Moreover, thanks to Lemma A.10, it suffices to show

$$P(|\hat{\theta}_{\hat{h}} - \theta^*| > 2A_T T^{-\gamma'}, \hat{h} \leq T^{-\gamma'}) \rightarrow 0.$$

On the event $\hat{h} \leq T^{-\gamma'}$, we have $\hat{h} \leq h^*(\gamma')$, so

$$|\hat{\theta}_{\hat{h}} - \theta^*| \leq |\hat{\theta}_{\hat{h}} - \hat{\theta}_{h^*(\gamma')}| + |\hat{\theta}_{h^*(\gamma')} - \theta^*| \leq A_T h^*(\gamma') + |\hat{\theta}_{h^*(\gamma')} - \theta^*| \leq A_T T^{-\gamma'} + |\hat{\theta}_{h^*(\gamma')} - \theta^*|,$$

where the second inequality follows by the definition of \hat{h} . Therefore,

$$P(|\hat{\theta}_{\hat{h}} - \theta^*| > 2A_T T^{-\gamma'}, \hat{h} \leq T^{-\gamma'}) \leq P(|\hat{\theta}_{h^*(\gamma')} - \theta^*| > A_T T^{-\gamma'}).$$

Since $P(|\hat{\theta}_{h^*(\gamma')} - \theta^*| > A_T T^{-\gamma'}) \rightarrow 0$ by Theorem 4.1, we obtain the desired result. \square

A.6 Proof of Theorem 4.3

The proof of Theorem 4.3 relies on Theorem 2.2 in [69], which requires the notion of the Hellinger distance. Recall that the Hellinger distance between two probability measures P and Q defined on a common measurable space $(\mathcal{X}, \mathcal{A})$ is defined as

$$H(P, Q) := \sqrt{\int_{\mathcal{X}} \left(\sqrt{\frac{dP}{d\nu}} - \sqrt{\frac{dQ}{d\nu}} \right)^2 d\nu},$$

where ν is any σ -finite measure on $(\mathcal{X}, \mathcal{A})$ dominating both P and Q . By Lemmas 2.9 and 2.10(1) in [66],

$$H^2(P, Q) = 2 \left(1 - \int_{\mathcal{X}} \sqrt{\frac{dQ}{dP}} dP \right), \quad (\text{A.29})$$

where $dQ/dP := dQ^a/dP$ with Q^a the absolutely continuous part of Q with respect to P . Note that Strasser [66] defines the Hellinger distance as $H(P, Q)/\sqrt{2}$ in our notation.

Proof of Theorem 4.3. Define a point process \tilde{N} on \mathbb{R}^2 as $\tilde{N} := \sum_{i=1}^{\infty} \delta_{(t_i, t_i + \gamma_i)}$. Since $N_1(\cdot) = \tilde{N}(\cdot \times \mathbb{R})$ and $N_2(\cdot) = \tilde{N}(\mathbb{R} \times \cdot)$, we have $\sigma(N \cap [0, T]) \subset \sigma(\tilde{N} \cap [0, T]^2)$. Also, with $D_T := [0, T] \times [-1, T + 1]$, we evidently have $\sigma(\tilde{N} \cap [0, T]^2) \subset \sigma(\tilde{N} \cap D_T)$. Therefore, it suffices to show that there exists a constant $b > 0$ such that

$$\liminf_{T \rightarrow \infty} \inf_{\hat{\theta}_T} \sup_{|\theta| \leq 2\rho_T} \sup_{g \in \mathcal{G}(\theta, \alpha, 1/2, b)} P_g \left(|\tilde{\theta}_T - \theta| \geq \rho_T \right) > 0, \quad (\text{A.30})$$

where the infimum is taken over all estimators based on $\tilde{N} \cap D_T$. For every probability density g on \mathbb{R} , we denote by $P_{T,g}$ the law of $\tilde{N} \cap D_T$ induced on $(\mathcal{N}_{D_T}^{\#}, \mathcal{B}(\mathcal{N}_{D_T}^{\#}))$ under P_g , where $\mathcal{N}_{D_T}^{\#}$ denotes the

space of all counting measures on D_T equipped with the $w^\#$ -topology; see [23, Appendix A2.6] and [24, Definition 9.1.II] for details. According to Eq.(2.9) and Theorem 2.2 in [69], we obtain (A.30) once we find $g_T \in \mathcal{G}(2\rho_T, \alpha, 1/2, b)$ and $g_0 \in \mathcal{G}(0, \alpha, 1/2, b)$ such that

$$\limsup_{T \rightarrow \infty} H^2(P_{T,g_T}, P_{T,g_0}) < 2. \quad (\text{A.31})$$

Let us compute $H^2(P_{T,g_T}, P_{T,g_0})$. Observe that \tilde{N} can be viewed as a cluster process on \mathbb{R} with centre process N_1 and component processes $\{\delta_{(t_i, t_i + \gamma_i)} : i \in \mathbb{N}\}$. Hence, by Proposition 6.3.III in [23], the probability generating functional (p.g.fl) of \tilde{N} under P_g for $g \in \{g_0, g_T\}$ is given by

$$\begin{aligned} G_g(\varphi) &= \exp \left(- \int_{\mathbb{R}} \left(1 - \int_{\mathbb{R}} \varphi(x, y) g(y - x) dy \right) dx \right) \\ &= \exp \left(\int_{\mathbb{R}^2} (\varphi(x, y) - 1) g(y - x) dx dy \right) \end{aligned}$$

for every measurable function $\varphi : \mathbb{R}^2 \rightarrow (0, 1]$ such that the support of $1 - \varphi$ is bounded. Since g is supported on $[-1, 1]$,

$$G_g(1 - 1_{D_T} + \varphi 1_{D_T}) = e^{-T} \exp \left(\int_{[0,T] \times \mathbb{R}} \varphi(x, y) g(y - x) dx dy \right).$$

Therefore, in view of Eq.(5.5.14) in [23], the local Janossy densities of \tilde{N} on D_T under P_g are given by

$$j_{n,g}((x_1, y_1), \dots, (x_n, y_n) \mid D_T) = e^{-T} \prod_{i=1}^n g(y_i - x_i) 1_{[0,T]}(x_i) \quad (n = 1, 2, \dots).$$

This gives

$$\frac{dP_{T,g_T}}{dP_{T,g_0}}(\tilde{N}) = \prod_{i: t_i \in [0,T]} \frac{g_T(\gamma_i)}{g_0(\gamma_i)} \quad P_{g_0}\text{-a.s.}$$

Here, recall that $dP_{T,g_T}/dP_{T,g_0} := dP_{T,g_T}^a/dP_{T,g_0}$ with P_{T,g_T}^a the absolutely continuous part of P_{T,g_T} with respect to P_{T,g_0} . Thus, by (A.29),

$$H^2(P_{T,g_T}, P_{T,g_0}) = 2 \left(1 - \mathbb{E}_{g_0} \left[\prod_{i: t_i \in [0,T]} \sqrt{\frac{g_T(\gamma_i)}{g_0(\gamma_i)}} \right] \right) =: 2(1 - a_T),$$

where \mathbb{E}_{g_0} denotes expectation under P_{g_0} . Therefore, (A.31) follows once we show $\liminf_{T \rightarrow \infty} a_T > 0$. Recall that under P_{g_0} , $(\gamma_i)_{i=1}^\infty$ is i.i.d. with common density g_0 and independent of N_1 . Hence,

$$a_T = \mathbb{E}_{g_0} \left[\left(\int \sqrt{g_T(x) g_0(x)} dx \right)^{N_1([0,T])} \right].$$

Since $N_1([0, T])$ follows the Poisson distribution with intensity T under P_{g_0} ,

$$a_T = \exp \left(T \left(\int \sqrt{g_T(x) g_0(x)} dx - 1 \right) \right) = \exp \left(-\frac{T}{2} \int \left(\sqrt{g_T(x)} - \sqrt{g_0(x)} \right)^2 dx \right).$$

Therefore, we complete the proof once we show that there exists a constant $b > 0$ such that

$$\int \left(\sqrt{g_T(x)} - \sqrt{g_0(x)} \right)^2 dx = O(T^{-1}) \quad (\text{A.32})$$

for some $g_T \in \mathcal{G}(2\rho_T, \alpha, 1/2, b)$ and $g_0 \in \mathcal{G}(0, \alpha, 1/2, b)$.

Case 1: $0 < \alpha < 1$. For every $\theta \in [0, 1]$, define a function $f_\theta : \mathbb{R} \rightarrow [0, \infty)$ as

$$f_\theta(x) = \alpha|x - \theta|^{\alpha-1}1_{[-1,0)}(x - \theta) \quad (x \in \mathbb{R}).$$

By construction, we evidently have $f_\theta \in \mathcal{G}(\theta, \alpha, 1/2, b)$ for some constant $b > 0$ depending only on α . Moreover, since f_0 satisfies Eq.(1.9) of [46, Chapter VI] in a neighborhood of $z = 0$ with $\alpha = \alpha - 1$, $p \equiv 1$ and $q \equiv 0$ in their notation, f_0 has one singularity of order $\alpha - 1$ located at 0 in the sense of Definition 1.1 of [46, Chapter VI]. Therefore, Theorem 1.1 in [46, Chapter VI] gives (A.32) for $g_T = f_{2\rho_T}$ and $g_0 = f_0$.

Case 2: $\alpha > 1$. We employ a minor variant of the construction used in the proof of [3, Theorem 2]. For every $\theta \in [0, 1/2)$, define functions $\psi_\theta : \mathbb{R} \rightarrow \mathbb{R}$ and $f_\theta : \mathbb{R} \rightarrow \mathbb{R}$ as

$$\psi_\theta(x) = (|x|^{\alpha-1} - (2\theta)^{\alpha-1})1_{(-2\theta,0]}(x) + (|x|^{\alpha-1} + (2\theta)^{\alpha-1} - 2^\alpha|x - \theta|^{\alpha-1})1_{(0,2\theta)}(x), \quad x \in \mathbb{R}$$

and

$$f_\theta(x) = \frac{\alpha}{2(\alpha - 1)} (1 - |x|^{\alpha-1} + \psi_\theta(x))1_{[-1,1]}(x), \quad x \in \mathbb{R}.$$

Observe that $f_\theta \geq 0$ and

$$\int_{-\infty}^{\infty} f_\theta(x)dx = \frac{\alpha}{2\alpha - 1} \left(\int_{-1}^1 (1 - |x|^{\alpha-1})dx + \int_{-2\theta}^{2\theta} |x|^{\alpha-1}dx - 2^\alpha \int_0^{2\theta} |x - \theta|^{\alpha-1}dx \right) = 1.$$

Hence f_θ is a probability density function on \mathbb{R} . Moreover, we have for all $x \in [-1, 1]$

$$2^{2-\alpha}|x - \theta|^{\alpha-1} \leq \frac{2(\alpha - 1)}{\alpha} (f_\theta(\theta) - f_\theta(x)) \leq 2^\alpha|x - \theta|^{\alpha-1}. \quad (\text{A.33})$$

In fact, a straightforward computation shows

$$\frac{2(\alpha - 1)}{\alpha} (f_\theta(\theta) - f_\theta(x)) = \begin{cases} 2(2\theta)^{\alpha-1} & \text{if } -2\theta < x \leq 0, \\ 2^\alpha|x - \theta|^{\alpha-1} & \text{if } 0 < x < 2\theta, \\ |x|^{\alpha-1} + (2\theta)^{\alpha-1} & \text{otherwise.} \end{cases}$$

Hence (A.33) is evident if $0 < x < 2\theta$. If $-2\theta < x \leq 0$, then $\theta \leq |x - \theta| \leq 3\theta$, so $2(2\theta)^{\alpha-1} \leq 2^\alpha|x - \theta|^{\alpha-1}$ and $2(2\theta)^{\alpha-1} \geq 2(2|x - \theta|/3)^{\alpha-1} \geq 2^{2-\alpha}|x - \theta|^{\alpha-1}$. Hence (A.33) holds. Also, Jensen's inequality gives $|x - \theta|^{\alpha-1} \leq 2^{\alpha-2}(|x|^{\alpha-1} + \theta^{\alpha-1}) \leq 2^{\alpha-2}(|x|^{\alpha-1} + (2\theta)^{\alpha-1})$. Hence the lower bound of (A.33) holds if $|x| \geq 2\theta$. Moreover, if $x \leq -2\theta$, then $|x| \geq 2\theta$ and $|x - \theta| = \theta - x \geq -x = |x|$, so

$$|x|^{\alpha-1} + (2\theta)^{\alpha-1} \leq 2|x|^{\alpha-1} \leq 2|x - \theta|^{\alpha-1}.$$

If $x \geq 2\theta$, then $x - \theta \geq \theta$ and thus

$$|x|^{\alpha-1} + (2\theta)^{\alpha-1} \leq 2^{\alpha-2}|x - \theta|^{\alpha-1} + 3 \cdot 2^{\alpha-2}\theta^{\alpha-1} \leq 2^\alpha|x - \theta|^{\alpha-1},$$

where the first inequality is by Jensen's inequality. Therefore, the upper bound of (A.33) also holds if $|x| \geq 2\theta$. Consequently, $f_\theta \in \mathcal{G}(\theta, \alpha, 1/2, b)$ for some constant $b > 0$ depending only on α .

Now, Eq.(2.27) of [69] gives

$$\begin{aligned} \int \left(\sqrt{f_\theta(x)} - \sqrt{f_0(x)} \right)^2 dx &\leq \int_{-1}^1 \left(\frac{f_\theta(x)}{f_0(x)} - 1 \right)^2 f_0(x) dx \\ &= \frac{\alpha}{2(\alpha-1)} \int_{-2\theta}^{2\theta} \frac{\psi_\theta(x)^2}{1-|x|^{\alpha-1}} dx \leq \frac{\alpha}{2(\alpha-1)} \frac{3(2\theta)^{2\alpha-1}}{1-(2\theta)^{\alpha-1}}. \end{aligned}$$

Hence (A.32) holds for $g_T = f_{2\rho_T}$ and $g_0 = f_0$. \square

A.7 Proof of Assumption [A2](ii) for LBHPG with gamma kernels

In this section, we show that LBHPG with common rate parameters $\beta_{ij} \equiv \beta > 0, i, j = 1, 2$ satisfies [A2](ii) with $\alpha = \min\{D_{12}, D_{21}\}$ when $\min\{D_{12}, D_{21}\} < 1$ and the stationary assumption (spectral radius $\rho(\alpha)$ of the matrix α is smaller than 1) holds. Let

$$h_a(t) := \frac{\beta^a}{\Gamma(a)} t^{a-1} e^{-\beta t} \mathbf{1}_{(0,\infty)}(t), \quad t \in \mathbb{R}, a > 0,$$

$\mathbf{H} = (h_{D_{ij}})_{1 \leq i, j \leq 2}$, $\alpha_* = \min\{D_{12}, D_{21}\} (< 1)$, and $D_* = \min\{D_{11}, D_{12}, D_{21}, D_{22}\}$. Then, we have $\Phi = \alpha \odot \mathbf{H}$ by definition, where \odot is the Hadamard product. Recall $\Psi = \sum_{m \geq 1} \Phi^{(*m)}$ converges in $L^1(\mathbb{R})$ componentwise.

By (5.1) and (5.2), it is sufficient to show the following proposition:

Proposition A.1. *Under the assumptions above, there exist $C > 0$ and $\delta > 0$ such that*

$$\alpha_{ij} h_{D_{ij}}(u) \leq \Psi_{ij}(u), \quad u > 0, (i, j) \in \{(1, 2), (2, 1)\}, \quad (\text{A.34})$$

$$\max\{\Psi_{12}(u), \Psi_{21}(u)\} \leq C u^{\alpha_*-1}, \quad 0 < u < \delta, \quad (\text{A.35})$$

$$0 \leq \int_{\mathbb{R}} \Psi_{i1}(s) \Psi_{i2}(s+u) ds \leq C |u|^{\alpha_*-1}, \quad 0 < |u| < \delta, i \in \{1, 2\}. \quad (\text{A.36})$$

In the following, we first provide several lemmas and then use them to establish Proposition A.1. Before proceeding, we decompose Ψ as

$$\Psi = \Psi^s + \Psi^b, \quad (\text{A.37})$$

where

$$\Psi^s := \sum_{m=1}^{M-1} \Phi^{(*m)}, \quad \Psi^b := \sum_{m=M}^{\infty} \Phi^{(*m)}, \quad M = \lceil 1/D_* \rceil + 1.$$

Lemma A.11. *For $m \geq 1$, $i, j \in \{1, 2\}$ and $t > 0$,*

$$(\Phi^{(*m)})_{ij}(t) = \sum_{\substack{(i_0, \dots, i_m) \in \{1, 2\}^{m+1}, \\ i_0 = j, i_m = i}} \left(\prod_{\ell=1}^m \alpha_{i_\ell i_{\ell-1}} \right) h_{\sum_{\ell=1}^m D_{i_\ell i_{\ell-1}}}(t).$$

Proof. The result follows from the gamma distribution's reproducibility. \square

Lemma A.12. *For every $a \geq 1$, $\|h_a\|_\infty \leq \beta$.*

Proof. Fix $a \geq 1$. Since the gamma density h_a is log-concave on $[0, \infty)$, we have

$$\|h_a\|_\infty \leq \frac{1}{\sigma_a}$$

by [61, Eq. (5.8)], where σ_a is the standard deviation of h_a . Since the standard deviation of h_a is $\sigma_a = \sqrt{a}/\beta$, we conclude that

$$\|h_a\|_\infty \leq \frac{\beta}{\sqrt{a}} \leq \beta.$$

□

Lemma A.13. *Each component of Ψ^b is bounded on \mathbb{R} .*

Proof. By Lemma A.11, for $m \geq M$ every component of $\Phi^{(*m)}$ is a gamma density with shape parameter at least $mD_* > 1$. Hence Lemma A.12 yields

$$\|(\Phi^{(*m)})_{ij}\|_\infty \leq \beta \sum_{\substack{(i_0, \dots, i_m) \in \{1, 2\}^{m+1}, \\ i_0=j, i_m=i}} \prod_{\ell=1}^m \alpha_{i_\ell i_{\ell-1}} = \beta(\boldsymbol{\alpha}^m)_{ij}.$$

Since $\rho(\boldsymbol{\alpha}) < 1$, the series $\sum_{m \geq 1} \boldsymbol{\alpha}^m$ converges entrywise, hence $\sum_{m \geq M} (\boldsymbol{\alpha}^m)_{ij} < \infty$ and therefore

$$\|\Psi_{ij}^b\|_\infty \leq \sum_{m=M}^{\infty} \|(\Phi^{(*m)})_{ij}\|_\infty \leq \beta \sum_{m \geq M} (\boldsymbol{\alpha}^m)_{ij} < \infty.$$

□

Proof of Proposition A.1. Throughout the proof, $C > 0$ and $\delta > 0$ denote generic constants.

Proof of (A.34). Since $\Psi = \sum_{m \geq 1} \Phi^{(*m)}$ and each term is nonnegative, we have $\Psi_{ij} \geq \Phi_{ij} = \alpha_{ij} h_{D_{ij}}$ on $(0, \infty)$, which yields (A.34).

Proof of (A.35). Fix $(i, j) \in \{(1, 2), (2, 1)\}$. By (A.37),

$$\Psi_{ij}(u) = \Psi_{ij}^s(u) + \Psi_{ij}^b(u), \quad u > 0.$$

By Lemma A.11 and the definition of Ψ^s as a finite sum, Ψ_{ij}^s is a finite nonnegative linear combination of gamma densities h_a (with common rate β) whose shape parameters satisfy $a \geq D_{ij} \geq \alpha_*$. Hence, there exists $C_s > 0$ such that $\Psi_{ij}^s(u) \leq C_s u^{\alpha_* - 1}$ for all $u \in (0, 1)$. Moreover, Lemma A.13 gives $\|\Psi_{ij}^b\|_\infty < \infty$. Choose $\delta \in (0, 1)$ so that $u^{\alpha_* - 1} \geq 1$ on $(0, \delta)$. Then for $u \in (0, \delta)$,

$$\Psi_{ij}(u) \leq C_s u^{\alpha_* - 1} + \|\Psi_{ij}^b\|_\infty \leq (C_s + \|\Psi_{ij}^b\|_\infty) u^{\alpha_* - 1}.$$

Taking the maximum over $(i, j) = (1, 2), (2, 1)$ yields (A.35).

Proof of (A.36). Fix $i \in \{1, 2\}$ and set

$$I_i(u) := \int_{\mathbb{R}} \Psi_{i1}(s) \Psi_{i2}(s+u) ds, \quad u \in \mathbb{R}.$$

Non-negativity implies $I_i(u) \geq 0$. We will prove the upper bound.

Using (A.37) and $\int_{\mathbb{R}} f(s)g(s+u) ds \leq \|f\|_1\|g\|_{\infty}$ for nonnegative f, g , we obtain

$$\begin{aligned} I_i(u) &= \int_{\mathbb{R}} (\Psi_{i1}^s + \Psi_{i1}^b)(s) (\Psi_{i2}^s + \Psi_{i2}^b)(s+u) ds \\ &\leq \int_{\mathbb{R}} \Psi_{i1}^s(s) \Psi_{i2}^s(s+u) ds + \|\Psi_{i1}\|_1 \|\Psi_{i2}^b\|_{\infty} + \|\Psi_{i1}^b\|_{\infty} \|\Psi_{i2}\|_1, \end{aligned}$$

where we used $\Psi_{ik}^s \leq \Psi_{ik}$ and $\Psi_{ik}^b \leq \Psi_{ik}$. Since $\|\Phi_{ij}\|_1 = \alpha_{ij}$ and $\|(\Phi^{(m)})_{ij}\|_1 = (\alpha^m)_{ij}$, the assumption $\rho(\alpha) < 1$ implies $\|\Psi_{ik}\|_1 = \sum_{m \geq 1} (\alpha^m)_{ik} < \infty$. By Lemma A.13, $\|\Psi_{ik}^b\|_{\infty} < \infty$. Hence, the last two terms are finite constants independent of u , and since $\alpha_* < 1$ we may shrink $\delta \in (0, 1)$ so that these constants are absorbed by $C|u|^{\alpha_*-1}$ on $0 < |u| < \delta$ (using $|u|^{\alpha_*-1} \geq 1$ there). Therefore, it suffices to show that

$$\int_{\mathbb{R}} \Psi_{i1}^s(s) \Psi_{i2}^s(s+u) ds \leq C|u|^{\alpha_*-1}, \quad 0 < |u| < \delta. \quad (\text{A.38})$$

For $a, b > 0$, define

$$f_{a,b}^{\text{BG}}(u) := \int_{\mathbb{R}} h_a(s) h_b(s+u) ds, \quad u \in \mathbb{R}.$$

Then, $f_{a,b}^{\text{BG}}$ is the probability density function of a bilateral gamma distribution [51] with parameters $(\alpha_+, \lambda_+, \alpha_-, \lambda_-) = (b, \beta, a, \beta)$. By Küchler & Tappe [51, Theorem 6.1], as $u \rightarrow 0$ the density satisfies $f_{a,b}^{\text{BG}}(u) = O(|u|^{a+b-1})$ if $a+b < 1$, and $f_{a,b}^{\text{BG}}(u) = O(M(|u|))$ if $a+b = 1$, where M is slowly varying at 0. If $a+b > 1$, then $f_{a,b}^{\text{BG}}$ is bounded in a neighborhood of 0. Consequently, for any $a, b > 0$ with $a+b > \alpha_*$, there exists $C_{a,b} > 0$ and $\delta_{a,b} \in (0, 1)$ such that

$$f_{a,b}^{\text{BG}}(u) \leq C_{a,b}|u|^{\alpha_*-1}, \quad 0 < |u| < \delta_{a,b} \quad (\text{A.39})$$

since $\alpha_* < 1$ by the assumption. Next, by Lemma A.11, each Ψ_{ik}^s is a finite nonnegative linear combination of gamma densities h_a . Hence, the left-hand side of (A.38) is a finite nonnegative linear combination of $f_{a,b}^{\text{BG}}(u)$. If $i = 1$, then Ψ_{12}^s only involves shapes $b \geq D_{12} \geq \alpha_*$, while shapes a in Ψ_{11}^s are strictly positive; thus $a+b > \alpha_*$. If $i = 2$, then Ψ_{21}^s only involves shapes $a \geq D_{21} \geq \alpha_*$, while shapes b in Ψ_{22}^s are strictly positive; thus again $a+b > \alpha_*$. Therefore, (A.39) applies to all pairs (a, b) appearing in the linear combination, we can take a common $\delta > 0$ and $C > 0$, which yields (A.38). This proves (A.36). \square

B Implementation and computational complexity

In this section, we discuss the efficient computation of the kernel density estimator $\hat{g}_h(u)$ and the search strategy for its maximizer $\hat{\theta}_h$. In our implementation, the expected time complexity for computing $\hat{\theta}_h$ from observations on $[0, T]$ with bandwidth h scales as

$$\begin{cases} O(T \log T + T^2 h), & \text{under Assumption [A2](i),} \\ O(T \log T + T^2 h^{\alpha}), & \text{under Assumption [A2](ii) with } 0 < \alpha < 1. \end{cases}$$

This is better than a naive $O(T^2)$ approach that evaluates $\hat{g}_h(u)$ at each candidate u by summing over all pairs, especially when the bandwidth h is small.

B.1 Algorithm for computing \hat{g}_h on a grid

Directly evaluating \hat{g}_h on a grid $\{u_1, \dots, u_M\} \subset \mathbb{R}$ may be computationally expensive, roughly scaling with the product of the grid size and the number of data pairs. To reduce computational cost, we employ an algorithm that iterates over relevant timestamp pairs and distributes their kernel weights onto nearby grid points. This approach is particularly efficient when the bandwidth h is small relative to the grid's range.

Let N_1 and N_2 be the underlying point processes, observed over the window $[0, T]$, and let $\mathcal{T}_i := \{t_{i,1} < \dots < t_{i,n_i}\} \subset [0, T]$, $n_i := N_i([0, T])$, $i = 1, 2$ denote the corresponding observed event times. Let $\mathcal{U} = \{u_1 < \dots < u_M\}$ be a sorted grid where we wish to evaluate the estimator, and define $u_{\min} := u_1$ and $u_{\max} := u_M$. For any $a < b$, define the set of relevant pairs in the lag window $[a, b]$ and the corresponding set of differences by

$$\mathcal{P}(a, b) := \{(x, y) \in \mathcal{T}_1 \times \mathcal{T}_2 : y - x \in [a, b]\}, \quad N_{\text{pairs}}(a, b) := |\mathcal{P}(a, b)|,$$

$$\mathcal{D}(a, b) := \{y - x : (x, y) \in \mathcal{P}(a, b)\} \subset [a, b].$$

Algorithm 1 outlines the procedure. Instead of fixing u and summing over all pairs, we iterate through each observed time $x \in \mathcal{T}_1$. Using binary search in \mathcal{T}_2 , we identify the range of $y \in \mathcal{T}_2$ for which the difference $d = y - x$ lies within the lag window $[u_{\min} - h, u_{\max} + h]$, i.e., the set of lags that can influence at least one grid point through a bandwidth- h kernel. For each such difference d , we find the subset of grid points in $\mathcal{U} \cap [d - h, d + h]$ (again via binary search) and accumulate the kernel contribution at those grid points. Throughout this section, we assume that K is supported on $[-1, 1]$.

Computational complexity. Only pairs in the lag window $[u_{\min} - h, u_{\max} + h]$ contribute to \hat{g}_h evaluated on \mathcal{U} , and the number of such pairs is $N_{\text{pairs}}(u_{\min} - h, u_{\max} + h)$. For each $x \in \mathcal{T}_1$, we locate the index range of $\mathcal{T}_2 \cap [x + u_{\min} - h, x + u_{\max} + h]$ by binary search in \mathcal{T}_2 , which costs $O(\log n_2)$ per x (and thus $O(n_1 \log n_2)$ in total). For each relevant pair $(x, y) \in \mathcal{P}(u_{\min} - h, u_{\max} + h)$ with $d = y - x$, we perform a binary search on \mathcal{U} to locate $\mathcal{U} \cap [d - h, d + h]$, which costs $O(\log M)$, and then update all grid points in that subarray. Let $M_h := \sup_{u \in \mathbb{R}} |\mathcal{U} \cap [u - h, u + h]|$ denote the maximum local grid occupancy at scale h . Thus, the total complexity is bounded by

$$O(n_1 \log n_2 + N_{\text{pairs}}(u_{\min} - h, u_{\max} + h)(\log M + M_h)).$$

This is significantly faster than the naive $O(M \cdot N_{\text{pairs}}(u_{\min} - h, u_{\max} + h))$ approach when $M_h \ll M$, which typically occurs when the bandwidth h is small. As suggested by Theorem 4.1, small bandwidths are desirable in practice, especially when g exhibits a sharp peak, where the proposed implementation yields a substantial computational gain.

B.2 Finding the maximizer of \hat{g}_h

To compute the estimator $\hat{\theta}_h$, we need to find the global maximizer of $\hat{g}_h(u)$ within the range $[-r, r]$. The objective function \hat{g}_h may have many local optima, making it difficult for standard numerical optimization to converge to the global maximum. However, when K is piecewise linear, $\hat{g}_h(u)$ is also piecewise linear.

Algorithm 1 Computation of $\hat{g}_h(u)$ on a grid

Require: Sorted event times $\mathcal{T}_1, \mathcal{T}_2$, sorted grid $\mathcal{U} = \{u_1, \dots, u_M\}$, bandwidth h , kernel K supported on $[-1, 1]$.

Ensure: Values $G = (G_1, \dots, G_M)$ corresponding to $(\hat{g}_h(u_1), \dots, \hat{g}_h(u_M))$.

Initialize $G \leftarrow (0, \dots, 0)$

$u_{\min} \leftarrow u_1, \quad u_{\max} \leftarrow u_M$

for $x \in \mathcal{T}_1$ **do**

 Identify indices $[j_{\text{start}}, j_{\text{end}}]$ for $\mathcal{T}_2 \cap [x + u_{\min} - h, x + u_{\max} + h]$

for $j \leftarrow j_{\text{start}}$ **to** j_{end} **do**

$y \leftarrow \mathcal{T}_2[j]$

$d \leftarrow y - x$

 Identify indices $[k_{\text{start}}, k_{\text{end}}]$ for $\mathcal{U} \cap [d - h, d + h]$

for $k \leftarrow k_{\text{start}}$ **to** k_{end} **do**

$G_k \leftarrow G_k + \frac{1}{h} K\left(\frac{d - u_k}{h}\right)$

end for

end for

end for

Scale G by $\frac{T}{n_1 n_2}$, i.e., $G \leftarrow \frac{T}{n_1 n_2} G$

return G

Hence, a maximizer over $[-r, r]$ can be found by evaluating \hat{g}_h only at the kink locations induced by the differences $d = y - x, x \in \mathcal{T}_1, y \in \mathcal{T}_2$.

Let $\mathcal{D}_{r,h} := \mathcal{D}(-r - h, r + h)$ denote the set of lag differences in the window $[-r - h, r + h]$. In particular, for the triangular kernel $K^{\text{tri}}(x) = (1 - |x|)\mathbf{1}_{[-1,1]}(x)$, the function may change slope only at $u = d - h, u = d, u = d + h$ for each lag difference $d \in \mathcal{D}_{r,h}$. Therefore, to obtain the maximizer $\hat{\theta}_h$, it suffices to evaluate \hat{g}_h on the candidate set

$$\mathcal{U}_{\text{kink}} := \left(\mathcal{D}_{r,h} \cup (\mathcal{D}_{r,h} + h) \cup (\mathcal{D}_{r,h} - h) \cup \{-r, r\} \right) \cap [-r, r].$$

In an implementation, it is recommended to remove duplicates in $\mathcal{U}_{\text{kink}}$ before sorting; otherwise the grid may contain repeated points and incur unnecessary work.

Computational complexity. The set $\mathcal{D}_{r,h}$ can be constructed while enumerating the relevant pairs $\mathcal{P}(-r - h, r + h)$, which takes $O(N_{\text{pairs}}(-r - h, r + h))$ time up to constant-factor overhead. Building $\mathcal{U}_{\text{kink}}$ from $\mathcal{D}_{r,h}$ is linear in $|\mathcal{U}_{\text{kink}}|$, and we may sort $\mathcal{U}_{\text{kink}}$ once to apply Algorithm 1. Evaluating \hat{g}_h on $\mathcal{U}_{\text{kink}}$ using Algorithm 1 has the same form as above, with M replaced by $|\mathcal{U}_{\text{kink}}|$ and with M_h defined as above but computed on the grid $\mathcal{U}_{\text{kink}}$:

$$O(n_1 \log n_2 + N_{\text{pairs}}(-r - h, r + h)(\log |\mathcal{U}_{\text{kink}}| + M_h)).$$

Finally, the maximizer is obtained by a single pass over the evaluated values, which costs $O(|\mathcal{U}_{\text{kink}}|)$.

Scaling in T and h . For the simple stationary bivariate point process $N = (N_1, N_2)$ with intensities λ_1, λ_2 and CPCF g , we have $E[n_i] = \lambda_i T$ for $i = 1, 2$. Moreover, by the definition of the cross-intensity function, we have

$$E[N_{\text{pairs}}(a, b)] = \int_{(0, T]^2} \mathbf{1}\{y - x \in [a, b]\} \lambda_{12}(y - x) dx dy \approx \lambda_1 \lambda_2 T \int_a^b g(u) du.$$

If $T \gg r + h$ and $[a, b] \subset [-r - h, r + h]$, then $E[N_{\text{pairs}}(a, b)] \asymp \lambda_1 \lambda_2 T \int_a^b g(u) du$. In particular,

$$E[N_{\text{pairs}}(-r - h, r + h)] = O(T), \quad E[n_1 \log n_2] = O(T \log T),$$

where the hidden constant depends on g through its mass on $[-r - h, r + h]$.

Next, note that $|\mathcal{U}_{\text{kink}}| \leq 3|\mathcal{D}_{r, h}| + 2 \leq 3N_{\text{pairs}}(-r - h, r + h) + 2$, so $|\mathcal{U}_{\text{kink}}| = O(T)$ in expectation, and the one-time sorting cost is $O(T \log T)$. For the local update cost on the kink grid, observe that for any $u \in [-r, r]$,

$$|\mathcal{U}_{\text{kink}} \cap [u - h, u + h]| \leq 3|\mathcal{D}_{r, h} \cap [u - 2h, u + 2h]| + 2 \leq 3N_{\text{pairs}}(u - 2h, u + 2h) + 2.$$

Taking expectations yields

$$E[|\mathcal{U}_{\text{kink}} \cap [u - h, u + h]|] = O\left(T \int_{u-2h}^{u+2h} g(v) dv\right).$$

Taking the supremum over $u \in [-r, r]$ gives the worst-case bound

$$M_h = O\left(T \sup_{u \in [-r, r]} \int_{u-2h}^{u+2h} g(v) dv\right).$$

In particular, if g is bounded (e.g., under [A2](i)), then $\int_{u-2h}^{u+2h} g(v) dv = O(h)$ uniformly in u , so $M_h = O(Th)$ and the expected time bound reduces to $O(T \log T + T^2 h)$. If g is unbounded at θ^* as in [A2](ii), then $\int_{\theta^*-2h}^{\theta^*+2h} g(v) dv = O(h^\alpha)$. Thus, we may have $M_h = O(Th^\alpha)$, leading to an expected time bound of $O(T \log T + T^2 h^\alpha)$. On the other hand, the naive implementation costs $O(N_{\text{pairs}} \times |\mathcal{U}_{\text{kink}}|) \approx O(T^2)$.

C Bandwidth selection by cross-validation

In this section, we introduce additional bandwidth-selection methods for the estimator $\hat{\theta}_h$ based on cross-validation and assess their performance in simulation studies.

In the context of modal regression, Chen *et al.* [19] propose choosing the bandwidth by minimizing the size of prediction sets associated with the modal regression function, while Zhou & Huang [72] introduce a cross-validation criterion (CVM) that penalizes the squared distance between the responses and the estimated modal set and includes an explicit penalty for the number of modes. Motivated by these developments, we design a cross-validation scheme that directly evaluates how well the maximizer set obtained from the training part of the point process predicts the empirical lag differences observed in the test part.

Fix an integer $K_{\text{cv}} \geq 2$ and split the observation window $[0, T]$ into K_{cv} disjoint subintervals $I_1, \dots, I_{K_{\text{cv}}}$ of equal length. Here K_{cv} denotes the number of folds. For the j th fold, we regard I_j as a test interval and

$[0, T] \setminus I_j$ as the corresponding training interval. On the training interval we compute the kernel estimator $\hat{g}_h^{(-j)}$ based on $N \cap ([0, T] \setminus I_j)$ and its (possibly set-valued) maximizer set

$$M_h^{(-j)} := \arg \max_{u \in [-r, r]} \hat{g}_h^{(-j)}(u), \quad h \in \mathcal{H}_T,$$

where \mathcal{H}_T is the finite bandwidth grid.

For a set $M \subset [-r, r]$ and $z \in \mathbb{R}$ we write

$$d(z, M) := \inf_{u \in M} |z - u|$$

for the distance from z to M . Given a test interval I_j , we define the set of observed lag differences restricted to $[-r, r]$ by

$$\Delta_j(r) := \{y - x; x \in \mathcal{T}_{1,j}, y \in \mathcal{T}_{2,j}, -r \leq y - x \leq r\},$$

where $\mathcal{T}_{i,j}$ denotes the (finite) set of event times of N_i that fall in I_j for $i \in \{1, 2\}$. We interpret $\Delta_j(r)$ as a multiset, i.e., lag differences are counted with multiplicity, and write $n_j := |\Delta_j(r)|$ for the number of elements. In practice, the fold length should be chosen large relative to r so that each I_j contains enough pairs with lag in $[-r, r]$. When $n_j \geq 1$, we enumerate the elements of $\Delta_j(r)$ as $(d_{j,1}, \dots, d_{j,n_j})$ (in an arbitrary order) and introduce the distances

$$\delta_{j,\ell}(M) := d(d_{j,\ell}, M), \quad \ell = 1, \dots, n_j,$$

with order statistics $\delta_{j,(1)}(M) \leq \dots \leq \delta_{j,(n_j)}(M)$. Fix a trimming parameter $\tau \in (0, 1]$ and a minimum count $n_{\min} \in \mathbb{N}$, and set

$$k_j := \max\{\lceil \tau n_j \rceil, n_{\min}\}, \quad \varepsilon_j(M) := \begin{cases} \delta_{j,(k_j)}(M), & n_j \geq k_j, \\ +\infty, & n_j < k_j. \end{cases}$$

If $n_j < k_j$, we set $L_{\text{nearest}}(M; I_j) = +\infty$, regardless of M , effectively discarding bandwidths for which the test fold contains too few lag differences. Under this notation, we consider the following loss functions on I_j for a finite candidate maximizer set $M \subset [-r, r]$ (so $|M|$ is its cardinality):

- **MSE-type loss:**

$$L_{\text{mse}}(M; I_j) := \frac{|M|^2}{n_j} \sum_{\ell=1}^{n_j} \delta_{j,\ell}(M)^2,$$

with the convention that folds with $n_j = 0$ are excluded from the CV average. The factor $|M|^2$ penalizes bandwidths that produce many maximizers, playing a stabilizing role in the spirit of Zhou & Huang [72].

- **Nearest-range loss:**

$$L_{\text{nearest}}(M; I_j) := \text{Leb}(\{x \in \mathbb{R} : d(x, M) \leq \varepsilon_j(M)\}).$$

The set $\{x \in \mathbb{R} : d(x, M) \leq \varepsilon\}$ is the ε -neighborhood of M , and $\text{Leb}(\cdot)$ is its total length. By construction, $\varepsilon_j(M)$ is chosen so that at least $k_j = \max\{\lceil \tau n_j \rceil, n_{\min}\}$ of the test lag differences lie

within distance $\varepsilon_j(M)$ of M , so $L_{\text{nearest}}(M; I_j)$ is the length of the smallest neighborhood of M covering that trimmed fraction. The minimum count n_{\min} improves numerical stability. This loss function is based on the prediction set approach of Chen *et al.* [19].

Let $J := \{j \in \{1, \dots, K_{\text{cv}}\} : n_j \geq 1\}$ denote the set of folds with at least one lag difference in $[-r, r]$. Given a choice of loss function $L \in \{L_{\text{mse}}, L_{\text{nearest}}\}$, we define the K_{cv} -fold CV score for $h \in \mathcal{H}_T$ by

$$\text{CV}(h) := \frac{1}{|J|} \sum_{j \in J} L(M_h^{(-j)}; I_j).$$

Our cross-validated bandwidth is then chosen as

$$\hat{h}_{\text{CV}} \in \arg \min_{h \in \mathcal{H}_T} \text{CV}(h)$$

If the minimizer is not unique, we select the smallest h in \mathcal{H}_T . We finally obtain the adaptive estimator $\hat{\theta}_{\hat{h}_{\text{CV}}}$.

To compare the performance of different loss functions and their accompanying tuning parameters, we conduct a series of simulation experiments under the following common design. The candidate bandwidths are $h \in \{10^{-1}, 10^{-2}, 10^{-3}, 10^{-4}, 10^{-5}, 10^{-6}\}$, $r = 1$, and the observation window is $[0, T]$. The observation horizon takes the values $T \in \{1000, 2000, 4000, 8000\}$; for each combination of model, estimator, and T , we generate 5000 Monte Carlo replicates. The cross-validation criteria considered are the nearest-range loss L_{nearest} with trimming levels $\tau \in \{0.01, 0.025, 0.05\}$ and the MSE-type loss L_{mse} . For comparison, we also include the Lepski selector with $A_T = \log \log T$. In the plots, the nearest-range CV curves for different τ are distinguished by a red color gradient; the MSE-based CV curves are shown in blue; and the curve of the Lepski estimator is shown in green. We set $K_{\text{cv}} = 5$ and $n_{\min} = 5$. For reference, each panel also shows the theoretical rate T^{-1/β_α} as a black dashed line.

Figure 6 compares the finite-sample performance of the different bandwidth selection schemes across the six data-generating models described in Section 5.1. Several systematic patterns emerge.

First, the cross-validation criterion based on the MSE-type loss is somewhat unstable. In five out of the six models, the RMSE of the MSE-CV estimator decreases only slowly, and sometimes not at all, as T increases, compared to the theoretical slope. This suggests that the MSE-type loss is not well-suited to selecting the bandwidth for our cases.

The nearest-range loss L_{nearest} behaves more favorably, but its performance depends on the trimming parameter τ . For models with sharper CPCFs, i.e., with α smaller than 1, smaller values of τ tend to work better. In contrast, for smoother models with $\alpha > 1$, larger values of τ become competitive or even preferable. In other words, the optimal choice of τ appears to be α -dependent: aggressive trimming is beneficial when g has a very sharp peak, whereas milder trimming is adequate when g is flatter around its maximum. A notable exception is the asymmetric Hawkes model (`hawkes_gamma_asym`). In this case, the nearest-range CV estimator improves more slowly and less regularly with T across the τ -values considered. One possible contributing factor is that L_{nearest} is built from symmetric neighborhoods of the estimated maximizer set, while the within-fold lag differences in this asymmetric setting may be skewed in finite samples; in such cases, symmetric neighborhoods may be less informative for selecting h .

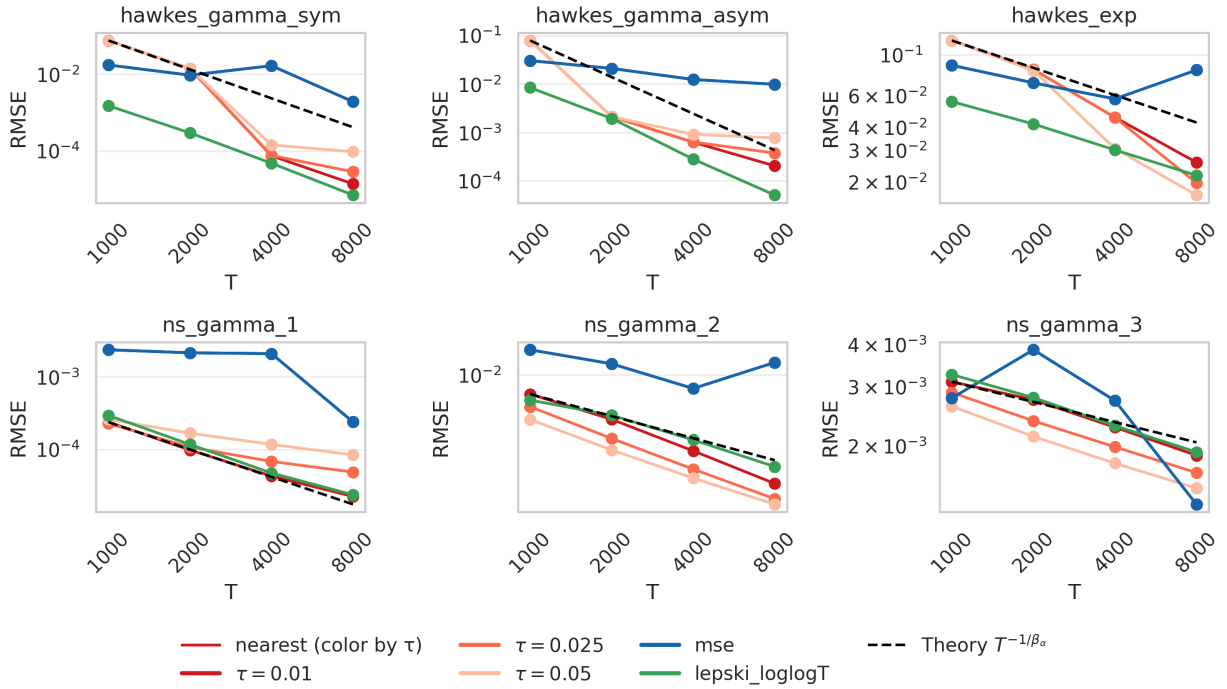


Figure 6: Performance comparisons between the bandwidth-selection methods across scenarios: RMSE versus T on log–log axes for CV using L_{nearest} (red gradient by τ), CV using L_{mse} (blue), and Lepski’s method with $A_T = \log \log T$ (green); the dashed black line shows the theoretical rate T^{-1/β_α} .

When compared with the Lepski-type procedure, the nearest-range CV estimator is inferior in the small- α models. Indeed, for `hawkes_gamma_sym`, `hawkes_gamma_asym`, and `ns_gamma_1`, the Lepski estimator shows lower RMSE. For smoother models with $\alpha > 1$, however, the best-tuned nearest-range CV estimator becomes competitive. Overall, these experiments indicate that cross-validation based on L_{nearest} is a promising alternative, but it may require a delicate choice of τ .

Taken together, our findings suggest the following practical recommendation. Among the bandwidth selectors we have examined, the Lepski method stands out as the most robust option. It requires only the slowly diverging threshold A_T , shows stable behavior across all models, and nearly attains the minimax rate T^{-1/β_α} both theoretically and in numerical experiments. Nearest-range cross-validation can be competitive, especially for smoother CPCFs, but it requires choosing the trimming level τ in addition to the bandwidth, and its best choice is not yet well understood theoretically. For this reason, we currently recommend the Lepski-type bandwidth choice as a default method for estimating the lead-lag time.

Acknowledgements We thank participants at the “Big Data and Artificial Intelligence in Econometrics, Finance, and Statistics” workshop at University of Chicago, October 2-4, 2025, the quantitative finance seminar at National University of Singapore, October 24, 2025, the KAKENHI symposium at Tsukuba University, October 30-31, 2025, Nakanoshima Workshop at Osaka University, December 5-6, 2025, and CFE-CMStatistics 2025 at University of London, December 13-15, 2025, for insightful comments and con-

structive suggestions on this work. Takaaki Shiotani's work was partly supported by Grant-in-Aid for JSPS Fellows (25KJ0933) and World-leading Innovative Graduate Study for Frontiers of Mathematical Sciences and Physics. Yuta Koike's work was partly supported by JST CREST Grant Number JPMJCR2115 and JSPS KAKENHI Grant Numbers JP22H00834, JP22H01139.

References

- [1] Abraham, C., Biau, G. & Cadre, B. (2003). Simple estimation of the mode of a multivariate density. *Canadian Journal of Statistics* **31**, 23–34.
- [2] Alsayed, H. & McGroarty, F. (2014). Ultra-high-frequency algorithmic arbitrage across international index futures. *Journal of Forecasting* **33**, 391–408.
- [3] Arias-Castro, E., Qiao, W. & Zheng, L. (2022). Estimation of the global mode of a density: Minimaxity, adaptation, and computational complexity. *Electronic Journal of Statistics* **16**, 2774–2795.
- [4] Bacry, E., Dayri, K. & Muzy, J.-F. (2012). Non-parametric kernel estimation for symmetric Hawkes processes. Application to high frequency financial data. *The European Physical Journal B* **85**, 157.
- [5] Bacry, E., Delattre, S., Hoffmann, M. & Muzy, J.-F. (2013). Some limit theorems for Hawkes processes and application to financial statistics. *Stochastic Processes and their Applications* **123**, 2475–2499.
- [6] Bacry, E., Mastromatteo, I. & Muzy, J.-F. (2015). Hawkes processes in finance. *Market Microstructure and Liquidity* **1**, 1550005.
- [7] Bangsgaard, C. & Kokholm, T. (2024). The lead–lag relation between VIX futures and SPX futures. *Journal of Financial Markets* **67**, 100851.
- [8] Bartlett III, R. P. & McCrary, J. (2019). How rigged are stock markets? Evidence from microsecond timestamps. *Journal of Financial Markets* **45**, 37–60.
- [9] Bercu, B., Gamboa, F. & Lavielle, M. (2002). Estimation of marginal and spectral modes. *Journal of Nonparametric Statistics* **14**, 353–366.
- [10] Bollen, N. P., O'Neill, M. J. & Whaley, R. E. (2017). Tail wags dog: Intraday price discovery in VIX markets. *Journal of Futures Markets* **37**, 431–451.
- [11] Boly, O., Cheysson, F. & Nguyen, T. H. (2023). Mixing properties for multivariate Hawkes processes. *arXiv preprint arXiv:2311.11730* .
- [12] Brillinger, D. R. (1972). The spectral analysis of stationary interval functions. In *Proceedings of the sixth berkeley symposium on mathematical statistics and probability, volume 1: Theory of statistics*, vol. 6. University of California Press, pp. 483–514.
- [13] Brillinger, D. R. (1975). Statistical inference for stationary point processes. In *Stochastic processes and related topics*. Academic Press, pp. 55–99.

- [14] Brillinger, D. R. (1976). Estimation of the second-order intensities of a bivariate stationary point process. *Journal of the Royal Statistical Society Series B: Statistical Methodology* **38**, 60–66.
- [15] Bryant Jr, H., Marcos, A. R. & Segundo, J. (1973). Correlations of neuronal spike discharges produced by monosynaptic connections and by common inputs. *Journal of Neurophysiology* **36**, 205–225.
- [16] Buccheri, G., Corsi, F. & Peluso, S. (2021). High-frequency lead-lag effects and cross-asset linkages: a multi-asset lagged adjustment model. *Journal of Business & Economic Statistics* **39**, 605–621.
- [17] Chacón, J. E. (2020). The modal age of statistics. *International Statistical Review* **88**, 122–141.
- [18] Chen, Y.-C. (2018). Modal regression using kernel density estimation: A review. *Wiley Interdisciplinary Reviews: Computational Statistics* **10**, e1431.
- [19] Chen, Y.-C., Genovese, C. R., Tibshirani, R. J. & Wasserman, L. (2016). Nonparametric modal regression. *Annals of Statistics* **44**, 489–514.
- [20] Cox, D. R. & Lewis, P. A. W. (1972). Multivariate point processes. In *Proceedings of the sixth berkeley symposium on mathematical statistics and probability*, vol. 3. University of California Press Berkeley, pp. 401–448.
- [21] Cucala, L. (2008). Intensity estimation for spatial point processes observed with noise. *Scandinavian Journal of Statistics* **35**, 322–334.
- [22] Da Fonseca, J. & Zaatour, R. (2017). Correlation and lead–lag relationships in a Hawkes microstructure model. *Journal of Futures Markets* **37**, 260–285.
- [23] Daley, D. J. & Vere-Jones, D. (2003). *An introduction to the theory of point processes*, vol. I: Elementary Theory and Methods. Springer, 2nd edn.
- [24] Daley, D. J. & Vere-Jones, D. (2008). *An introduction to the theory of point processes*, vol. II: General theory and structure. Springer, 2nd edn.
- [25] Dao, T. M., McGroarty, F. & Urquhart, A. (2018). Ultra-high-frequency lead–lag relationship and information arrival. *Quantitative Finance* **18**, 725–735.
- [26] De Jong, F. & Nijman, T. (1997). High frequency analysis of lead-lag relationships between financial markets. *Journal of Empirical Finance* **4**, 259–277.
- [27] Dobrev, D. & Schaumburg, E. (2015). High-frequency cross-market trading: Model free measurement and applications. Working paper.
- [28] Dobrev, D. & Schaumburg, E. (2023). High-frequency cross-market trading: Model free measurement and testable implications. Working paper.
- [29] Doukhan, P. (1994). *Mixing; properties and examples*. New York : Springer.

- [30] Doukhan, P. & Louhichi, S. (1999). A new weak dependence condition and applications to moment inequalities. *Stochastic Processes and their Applications* **84**, 313–342.
- [31] Eddy, W. F. (1980). Optimum kernel estimators of the mode. *Annals of Statistics* **8**, 870–882.
- [32] Ellis, S. P. (1991). Density estimation for point processes. *Stochastic Processes and their Applications* **39**, 345–358.
- [33] Giné, E. & Nickl, R. (2016). *Mathematical foundations of infinite-dimensional statistical models*, vol. 40 of *Cambridge Series in Statistical and Probabilistic Mathematics*. Cambridge University Press.
- [34] Guan, Y. (2007). A least-squares cross-validation bandwidth selection approach in pair correlation function estimations. *Statistics & Probability Letters* **77**, 1722–1729.
- [35] Hasbrouck, J. (2021). Price discovery in high resolution. *Journal of Financial Econometrics* **19**, 395–430.
- [36] Has'minskii, R. (1979). Lower bound for the risks of nonparametric estimates of the mode. In *Contributions to statistics*. D. Reidel Publishing Company, pp. 91–97.
- [37] Hayashi, T. (2017). Statistical analysis of high-frequency limit-order book data: On cross-market, single-asset lead-lag relationships in the Japanese stock market (in Japanese). *Proceedings of the Institute of Statistical Mathematics* **65**, 113–139.
- [38] Hayashi, T. & Koike, Y. (2018). Wavelet-based methods for high-frequency lead-lag analysis. *SIAM Journal on Financial Mathematics* **9**, 1208–1248.
- [39] Hayashi, T. & Koike, Y. (2020). Multi-scale analysis of lead-lag relationships in high-frequency financial markets. *arXiv preprint arXiv:1708.03992v4* .
- [40] Herrmann, E. & Ziegler, K. (2004). Rates of consistency for nonparametric estimation of the mode in absence of smoothness assumptions. *Statistics & Probability Letters* **68**, 359–368.
- [41] Hessellund, K. B., Xu, G., Guan, Y. & Waagepetersen, R. (2022). Second-order semi-parametric inference for multivariate log Gaussian Cox processes. *Journal of the Royal Statistical Society Series C: Applied Statistics* **71**, 244–268.
- [42] Hessellund, K. B., Xu, G., Guan, Y. & Waagepetersen, R. (2022). Semiparametric multinomial logistic regression for multivariate point pattern data. *Journal of the American Statistical Association* **117**, 1500–1515.
- [43] Hoffmann, M., Rosenbaum, M. & Yoshida, N. (2013). Estimation of the lead-lag parameter from non-synchronous data. *Bernoulli* **19**, 426–461.
- [44] Holden, C. W., Pierson, M. & Wu, J. (2023). In the blink of an eye: Exchange-to-SIP latency and trade classification accuracy. *Available at SSRN 4441422* .

- [45] Huth, N. & Abergel, F. (2014). High frequency lead/lag relationships—empirical facts. *Journal of Empirical Finance* **26**, 41–58.
- [46] Ibragimov, I. & Has'minskii, R. (1981). *Statistical estimation: Asymptotic theory*. Springer.
- [47] Jalilian, A. & Waagepetersen, R. (2018). Fast bandwidth selection for estimation of the pair correlation function. *Journal of Statistical Computation and Simulation* **88**, 2001–2011.
- [48] Jovanović, S., Hertz, J. & Rotter, S. (2015). Cumulants of Hawkes point processes. *Physical Review E* **91**, 042802.
- [49] Klemelä, J. (2005). Adaptive estimation of the mode of a multivariate density. *Journal of Nonparametric Statistics* **17**, 83–105.
- [50] Koike, Y. (2021). Inference for time-varying lead–lag relationships from ultra-high-frequency data. *Japanese Journal of Statistics and Data Science* **4**, 643–696.
- [51] Küchler, U. & Tappe, S. (2008). On the shapes of bilateral gamma densities. *Statistics & Probability Letters* **78**, 2478–2484.
- [52] Leblanc, T. (2024). Exponential moments for Hawkes processes under minimal assumptions. *Electronic Communications in Probability* **29**, 1–11.
- [53] Malliavin, P. (1995). *Integration and probability*, vol. 157 of *Graduate Texts in Mathematics*. Springer.
- [54] Meister, A. (2011). On general consistency in deconvolution mode estimation. *Journal of Statistical Planning and Inference* **141**, 771–781.
- [55] Parzen, E. (1962). On estimation of a probability density function and mode. *Annals of Mathematical Statistics* **33**, 1065–1076.
- [56] Pierson, M. & Wu, J. (2025). A latency commentary: Why dynamic RBBO outperforms fixed latency adjustment. *Available at SSRN 5185422* .
- [57] Poinas, A., Delyon, B. & Lavancier, F. (2019). Mixing properties and central limit theorem for associated point processes. *Bernoulli* **25**, 1724–1754.
- [58] Potiron, Y. & Volkov, V. (2025). Mutually exciting point processes with latency. *Journal of the American Statistical Association* , 1–22.
- [59] Poutré, C., Dionne, G. & Yergeau, G. (2024). The profitability of lead–lag arbitrage at high frequency. *International Journal of Forecasting* **40**, 1002–1021.
- [60] Rambaldi, M., Filimonov, V. & Lillo, F. (2018). Detection of intensity bursts using Hawkes processes: An application to high-frequency financial data. *Physical Review E* **97**, 032318.

- [61] Saumard, A. & Wellner, J. A. (2014). Log-concavity and strong log-concavity: A review. *Statistics surveys* **8**, 45–114.
- [62] Schwenk-Nebbe, S. (2024). *Big data finance*. Ph.D. thesis, Aarhus University.
- [63] Shaw, T., Møller, J. & Waagepetersen, R. P. (2021). Globally intensity-reweighted estimators for K -and pair correlation functions. *Australian & New Zealand Journal of Statistics* **63**, 93–118.
- [64] Sheather, S. J. & Jones, M. C. (1991). A reliable data-based bandwidth selection method for kernel density estimation. *Journal of the Royal Statistical Society: Series B (Methodological)* **53**, 683–690.
- [65] Shiotani, T. & Yoshida, N. (2024). Statistical inference for highly correlated stationary point processes and noisy bivariate Neyman-Scott processes. *arXiv preprint arXiv:2410.05732* .
- [66] Strasser, H. (1985). *Mathematical theory of statistics*. Walter de Gruyter & Co.
- [67] Tivnan, B. F., Dewhurst, D. R., Van Oort, C. M., Ring, J. H., Gray, T. J., Tivnan, B. F., Koehler, M. T. K., McMahon, M. T., Slater, D. M., Veneman, J. G. & Danforth, C. M. (2020). Fragmentation and inefficiencies in US equity markets: Evidence from the Dow 30. *PLoS ONE* **15**, e0226968.
- [68] Tivnan, B. F., Slater, D., Thompson, J. R., Bergen-Hill, T. A., Burke, C. D., Brady, S. M., Koehler, M. T., McMahon, M. T., Tivnan, B. F. & Veneman, J. G. (2018). Price discovery and the accuracy of consolidated data feeds in the US equity markets. *Journal of Risk and Financial Management* **11**, 73.
- [69] Tsybakov, A. B. (2009). *Introduction to nonparametric estimation*. Springer.
- [70] Vieu, P. (1996). A note on density mode estimation. *Statistics & Probability Letters* **26**, 297–307.
- [71] Wegman, E. J. (1971). A note on the estimation of the mode. *Annals of Mathematical Statistics* **42**, 1909–1915.
- [72] Zhou, H. & Huang, X. (2019). Bandwidth selection for nonparametric modal regression. *Communications in Statistics-Simulation and Computation* **48**, 968–984.